OXFORD

SOT | Society of Toxicology
www.toxsci.oxfordjournals.org

TOXICOLOGICAL SCIENCES, 2019, 1–15

doi: 10.1093/toxsci/kfz150
Advance Access Publication Date: July 3, 2019
Research Article

Atropselective Oxidation of 2,2′,3,3′,4,6′-Hexachlorobiphenyl (PCB 132) to Hydroxylated Metabolites by Human Liver Microsomes and Its Implications for PCB 132 Neurotoxicity

Eric Uwimana,[*,†] Brianna Cagle,[‡] Coby Yeung,[§] Xueshu Li,[*,†] Eric V. Patterson,[§] Jonathan A. Doorn,[‡] and Hans-Joachim Lehmler[*,†,1]

[*]Interdisciplinary Graduate Program in Human Toxicology and [†]Department of Occupational and Environmental Health, College of Public Health, University of Iowa Research Park, University of Iowa, Iowa City, Iowa 52242-5000; [‡]Department of Pharmaceutical Sciences and Experimental Therapeutics, College of Pharmacy, University of Iowa, Iowa City, Iowa 52242; and [§]Department of Chemistry, College of Arts and Sciences, Stony Brook University, Stony Brook, New York 11794–3400

[1]To whom correspondence should be addressed at Department of Occupational and Environmental Health, University of Iowa Research Park, University of Iowa, B164 MTF, Iowa City, IA 52242-5000. Fax: (319) 335-4290. E-mail: hans-joachim-lehmler@uiowa.edu.

ABSTRACT

Polychlorinated biphenyls (PCBs) have been associated with neurodevelopmental disorders. Several neurotoxic congeners display axial chirality and atropselectively affect cellular targets implicated in PCB neurotoxicity. Only limited information is available regarding the atropselective metabolism of these congeners in humans and their atropselective effects on neurotoxic outcomes. Here we investigate the hypothesis that the oxidation of 2,2′,3,3′,4,6′-hexachlorobiphenyl (PCB 132) by human liver microsomes (HLMs) and their effects on dopaminergic cells in culture are atropselective. Racemic PCB 132 was incubated with pooled or single donor HLMs, and levels and enantiomeric fractions of PCB 132 and its metabolites were determined gas chromatographically. The major metabolite was either 2,2′,3,4,4′,6′-hexachlorobiphenyl-3′-ol (3′-140), a 1,2-shift product, or 2,2′,3,3′,4,6′-hexachlorobiphenyl-5′-ol (5′-132). The PCB 132 metabolite profiles displayed interindividual differences and depended on the PCB 132 atropisomer. Computational studies suggested that 3′-140 is formed via a 3,4-arene oxide intermediate. The second eluting atropisomer of PCB 132, first eluting atropisomer of 3′-140, and second eluting atropisomer of 5′-132 were enriched in all HLM incubations. Enantiomeric fractions of the PCB 132 metabolites differed only slightly between the single donor HLM preparations investigated. Reactive oxygen species and levels of dopamine and its metabolites were not significantly altered after a 24 h exposure of dopaminergic cells to pure PCB 132 atropisomers. These findings suggest that there are interindividual differences in the atropselective biotransformation of PCB 132 to its metabolites in humans; however, the resulting atropisomeric enrichment of PCB 132 is unlikely to affect neurotoxic outcomes associated with the endpoints investigated in the study.

Key words: 1,2-shift; arene oxide; biotransformation; cytochrome P450 enzymes; dopamine metabolism; enantiomers; reactive oxygen species.

Polychlorinated biphenyl (PCB) congeners with a 2,3,6-chlorine substitution pattern on 1 phenyl ring, such as 2,2′,3,3′,4,6′-hexachlorobiphenyl (PCB 132), are important components of commercial PCB mixtures (Kania-Korwel and Lehmler, 2016a). Food is the major source of exposure to these and other PCB congeners (Schecter *et al.*, 2010; Su *et al.*, 2012; Voorspoels *et al.*, 2008). For example, PCB 132 has been detected in fish species caught for human consumption (Wong *et al.*, 2001). PCB 132 is also present in the indoor air of U.S. schools (Thomas *et al.*, 2012), raising concerns about inhalation exposure of school children, teachers, and staff to PCBs (Herrick *et al.*, 2016). PCB 132 and structurally related PCB congeners are present in human blood (DeCaprio *et al.*, 2005; Jursa *et al.*, 2006; Whitcomb *et al.*, 2005), breast milk (Bordajandi *et al.*, 2008; Bucheli and Brandli, 2006; Glausch *et al.*, 1995), and postmortem human tissue samples (Chu *et al.*, 2003). Like several other PCB congeners with a 2,3,6-chlorine substitution pattern, PCB 132 is axially chiral because it exists as 2 stable rotational isomers, or atropisomers, which are nonsuperimposable mirror images of each other (Lehmler *et al.*, 2010).

Exposure to PCBs has been implicated in the etiology of neurodevelopmental and neurodegenerative disorders (Hatcher-Martin *et al.*, 2012; Jones and Miller, 2008; Pessah *et al.*, 2010). In particular, PCB congeners with 2 or more *ortho* chlorine substituents are neurotoxic and, for example, have been associated with behavioral and cognitive deficits in animal models (Caudle *et al.*, 2006; Schantz *et al.*, 1995; Wayman *et al.*, 2012). Similarly, animal studies with hydroxylated PCB metabolites reported impairments in behavioral and locomotor activity in rats and mice (Haijima *et al.*, 2017; Lesmana *et al.*, 2014). Mechanistic studies suggest that these PCBs affect the dopaminergic system. *ortho*-Chlorinated PCBs inhibited dopamine uptake in rat synaptosomes (Mariussen and Fonnum, 2001) and decreased the dopamine content in cells in culture, possibly due to inhibition of dopamine synthesis (Seegal, 1996). 2,2′,3,4′,6-Pentachlorobiphenyl (PCB 91) and 2,2′,3,5′,6-pentachlorobiphenyl (PCB 95) decreased dopamine content in rat synaptosomes by inhibiting vesicular monoamine transporter (VMAT) (Bemis and Seegal, 2004). In contrast, PCB 95 increased intracellular dopamine and decreased dopamine in the medium by down-regulating VMAT2 expression in PC12 cells (Enayah *et al.*, 2018). Striatal dopamine levels in male mice exposed to PCB mixtures decreased due to a decrease in the expression of the dopamine transporter and VMAT2 (Richardson and Miller, 2004). Other studies suggest that, in addition to their effects on the dopaminergic system, PCB neurotoxicity can be mediated by altered intracellular Ca^{2+} signaling and/or disruption of thyroid and sex hormone homeostasis (reviewed by Kodavanti and Curras-Collazo, 2010; Mariussen and Fonnum, 2006; Pessah *et al.*, 2010).

Neurotoxic PCBs are metabolized to potentially neurotoxic hydroxylated metabolites (OH-PCBs, hydroxylated polychlorinated biphenyls) in animal models and humans (Grimm *et al.*, 2015; Kania-Korwel and Lehmler, 2016a). In general, PCB congeners with H-atoms in vicinal *meta* and *para* positions are readily metabolized by cytochrome P450 (P450) enzymes, whereas congeners without adjacent *para* and *meta* positions are metabolized more slowly (Grimm *et al.*, 2015). The oxidation of PCBs by P450 enzymes occurs by direct insertion of an oxygen atom into an aromatic C–H bond or via an arene oxide intermediate (Forgue and Allen, 1982; Forgue *et al.*, 1979; Preston *et al.*, 1983). Several P450 isoforms, including CYP2A and CYP2B enzymes, are involved in the metabolism of *ortho*-chlorinated PCB congeners, such as PCB 132, in different species (Lu *et al.*, 2013; McGraw and Waller, 2006; Nagayoshi *et al.*, 2018; Ohta *et al.*, 2012; Uwimana *et al.*, 2019; Waller *et al.*, 1999; Warner *et al.*, 2009). Hydroxylated and methyl sulfone metabolites of PCB 132 have been detected in human blood, breast milk, and feces (Haraguchi *et al.*, 2004, 2005). Similar to animal studies (Norstroem and Bergman, 2006), PCB 132 undergoes atropisomeric enrichment in humans (Bordajandi *et al.*, 2008; Bucheli and Brandli, 2006; Chu *et al.*, 2003; Glausch *et al.*, 1995; Zheng *et al.*, 2016) due to atropselective metabolism of PCB 132.

Biotransformation studies reveal species differences in the atropselective metabolism of PCBs to chiral hydroxylated metabolites (Kania-Korwel and Lehmler, 2016a); however, only a few PCB metabolism studies in humans have been reported (Schnellmann *et al.*, 1983; Uwimana *et al.*, 2016; 2018; Wu *et al.*, 2014). Because PCB 132 is present in the environment, displays atropisomeric enrichment in human samples, and represents a largely unexplored environmental and human health concern, the objective of this study was to investigate the atropselective metabolism of PCB 132 to OH-PCB metabolites by human liver microsomes (HLMs) and assess if PCB 132 atropselectively affects neurotoxic outcomes in dopaminergic cells in culture.

MATERIALS AND METHODS

Chemicals and materials. Sources and purities of racemic PCB 132 (Supplementary Table 1), PCB metabolite standards, chemicals, and other reagents; information regarding the HLM preparations; and a description of the separation and characterization of PCB 132 atropisomers are presented in the Supplementary Material. Gas chromatograms and the corresponding mass spectrum of PCB 132 are shown in Supplementary Figures 1 and 2. The chemical structures and abbreviations of OH-PCB 132 metabolites are shown in Figure 1. Rat-tail collagen was obtained from Sigma Aldrich (St Louis, Missouri). All other cell culture components such as fetal bovine serum (FBS), horse serum (HS), RPMI 1640 medium, and penicillin-streptomycin were obtained from Life Technologies (Carlsbad, California). 3,4-Dihydroxyphenylacetic acid (DOPAC) was obtained from Sigma Aldrich. Dihydroxyphenyl ethanol (DOPET) was obtained by reducing 3,4-dihydroxyphenylaldehyde (DOPAL) in a 10-fold excess of sodium borohydride (Jinsmaa *et al.*, 2009). DOPAL was obtained synthetically from epinephrine by the method of Fellman (Anderson *et al.*, 2011; Fellman, 1958).

Microsomal incubations. The metabolism of PCB 132 was investigated in an incubation system containing sodium phosphate buffer (0.1 M, pH 7.4), magnesium chloride (3 mM), pooled human liver microsomes (pHLMs), or single donor HLMs (0.1 mg/ml), and NADPH (1 mM) (Kania-Korwel *et al.*, 2011; Uwimana *et al.*, 2017; Wu *et al.*, 2011). The incubation mixtures were preincubated for 5 min, and PCB 132 (50 μM in DMSO; ≤ 0.5% vol/vol) was added to give a final volume of 2 ml. The mixtures were maintained for 10, 30, or 120 min at 37°C. Incubations with (−)-PCB 132, (+)-PCB132, or racemic PCB 132 (50 μM in DMSO; ≤ 0.5% vol/vol) were carried out analogously for 30 min at 37°C. The formation of PCB 132 metabolites was linear with time for up to 30 min. To terminate the enzymatic reaction, ice-cold sodium hydroxide (2 ml, 0.5 M) was added to each sample. Subsequently, the incubation mixtures were heated at 110°C for 10 min. Phosphate buffer blanks and control incubations without PCB accompanied each microsomal preparation. The following incubations were performed in parallel with each experiment to control for the abiotic transformation of PCB 132:

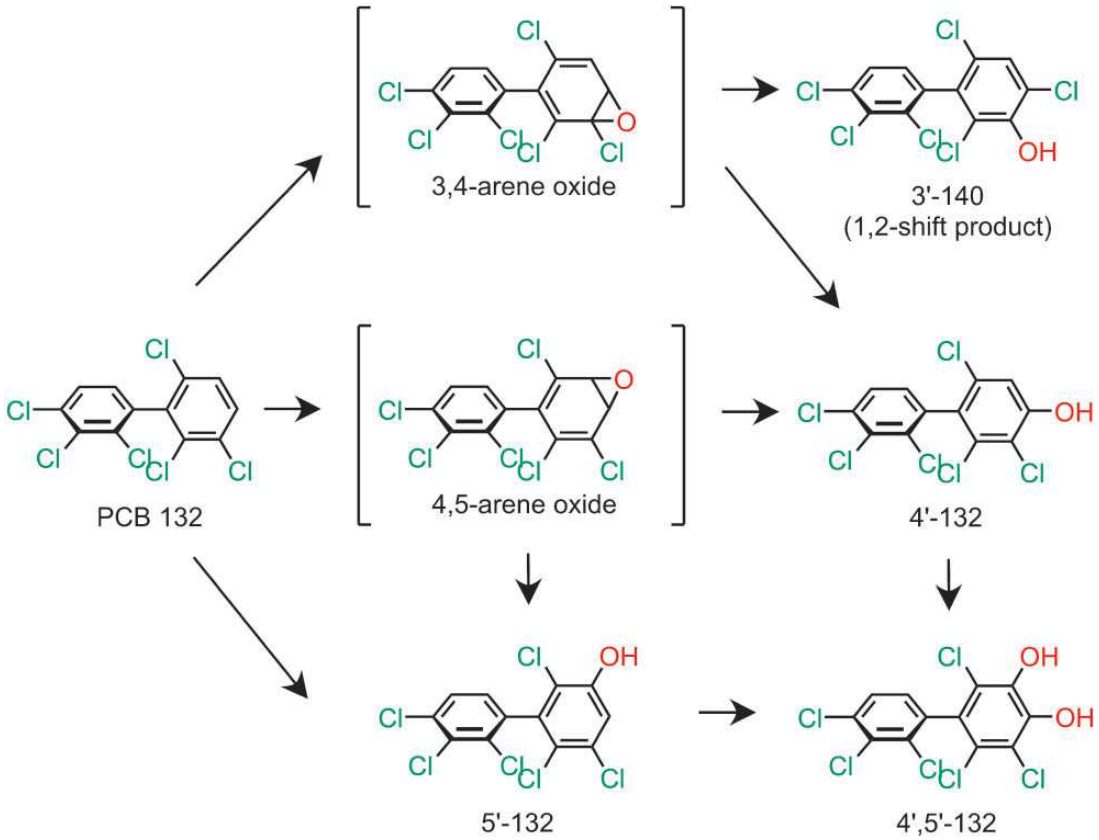

Figure 1. Proposed metabolism scheme showing the chemical structures of metabolites of PCB 132 identified in incubations with human liver microsomes (HLMs). Only 1 atropisomer of each metabolite is shown for clarity reasons. Abbreviations: PCB 132—2,2′,3,3′,4,6′-hexachlorobiphenyl; 3′-140—2,2′,3,4,4′,6′-hexachlorobiphenyl-3-ol; 4′-132—2,2′,3,3′,4,6′-hexachlorobiphenyl-4′-ol; 5′-132—2,2′,3,3′,4,6′-hexachlorobiphenyl-5′-ol; P450—cytochrome P450 enzymes.

Incubations without NADPH, without microsomes, and with heat-inactivated microsomes. No metabolites were detected in the control samples. All incubations were performed in triplicate, if not stated otherwise.

Extraction of PCB 132 and its hydroxylated metabolites. PCB 132 and its hydroxylated metabolites were extracted from the incubation mixtures as reported previously (Kania-Korwel *et al.*, 2011; Uwimana *et al.*, 2016; Wu *et al.*, 2011). Briefly, PCB 117 (200 ng) and 4′-159 (68.5 ng) were added to each sample as surrogate recovery standards, followed by hydrochloric acid (6 M, 1 ml) and 2-propanol (5 ml). The samples were extracted with a hexane-MTBE mixture (1:1 vol/vol, 5 ml) and re-extracted once with hexane (3 ml). The organic layers were washed with aqueous potassium chloride (1%, 4 ml), the organic phase was transferred to a new vial, and the KCl mixture was re-extracted with hexane (3 ml). The organic layers were evaporated to dryness under a gentle stream of nitrogen and reconstituted with hexane (1 ml). After derivatization with diazomethane (0.5 ml in diethyl ether) for approximately 16 h at 4°C (Kania-Korwel *et al.*, 2008), all extracts were subjected to sulfur and sulfuric acid clean-up steps before gas chromatographic analysis (Kania-Korwel *et al.*, 2005, 2007).

Identification of PCB 132 metabolites. The identity of the hydroxylated PCB 132 metabolites was confirmed by high-resolution gas chromatography with time-of-flight mass spectrometry (GC-TOF/MS) (Uwimana *et al.*, 2016; 2018). To obtain metabolite levels sufficient for GC-TOF/MS analysis, incubations were performed using the following experimental conditions: 50 μM racemic PCB 132, 0.3 mg/ml microsomal protein, and 1 mM NADPH for 90 min at 37°C. Metabolites were extracted and derivatized as described above before analysis on a Waters GCT Premier gas chromatograph (Waters Corporation, Milford, Massachusetts) combined with a time-of-flight mass spectrometer in the High-Resolution Mass Spectrometry Facility of the University of Iowa (Iowa City, Iowa) (Uwimana *et al.*, 2016; 2018). Measurements were performed with and without heptacosafluorotributylamine as lock mass to determine the accurate mass of $[M]^+$ and obtain mass spectra of the metabolites. PCB 132 metabolites were identified using the following criteria: The average relative retention times (RRT) of the OH-PCB 132 metabolites, calculated relative to PCB 51 as internal standard, were within 0.5% of the RRT of the authentic standard (European Commission, 2002); experimental accurate mass determinations were within 0.003 Da of the theoretical mass of $[M]^+$; and the deviation between experimental and theoretical isotope pattern of $[M]^+$ was $< 20\%$.

Quantification of PCB 132 metabolite levels. Levels of OH-PCB 132 metabolites in extracts were quantified as methylated derivatives on an Agilent 7890A gas chromatograph with a ^{63}Ni-micro electron capture detector (μECD) and a SPB-1 capillary column (60 m length, 250 μm inner diameter, 0.25 μm film thickness; Supelco, St Louis, Missouri) as reported earlier (Uwimana *et al.*, 2016, 2017; Wu *et al.*, 2013b). PCB 204 was added as internal standard (volume corrector) prior to analysis, and concentrations of OH-PCB 132 metabolites (as methylated derivatives) were

determined using the internal standard method (Kania-Korwel *et al.*, 2011; Wu and Lehmler, 2016; Wu *et al.*, 2011). Levels of PCB and its metabolites were not adjusted for recovery to facilitate a comparison with earlier studies (Uwimana *et al.*, 2016, 2018, 2019; Wu and Lehmler, 2016). The average RRTs of the metabolites, calculated relative to PCB 204, were within 0.5% of the RRT for the respective standard (European Commission, 2002). Metabolite levels and formation rates for all experiments described in the manuscript are summarized in the Supplementary Tables 2–4.

Ring opening calculations. The ring opening reactions of selected PCB arene oxide intermediates were modeled using density functional theory at the M11/def2-SVP level of theory (Peverati and Truhlar, 2011; Weigend and Ahlrichs, 2005), coupled with the SMD aqueous continuum solvation model (Marenich *et al.*, 2009), to assess if the formation of specific OH-PCB metabolites is energetically favored. The reactions were examined under neutral conditions, with 2 explicit water molecules complexed to the system to serve as a proton shuttle. To ascertain steric and electronic effects, calculations were carried out on arene oxides formed from 1,2,4-trichlorobenzene (TCB), 2,3,6-trichlorobiphenyl, PCB 91, PCB 95, PCB 132, and PCB 136. Transition states were characterized by normal mode analysis and confirmed via intrinsic reaction coordinate (IRC) calculations. All calculations were performed using Gaussian 16, Rev. A.01 (Frisch *et al.*, 2016). Additional details including computational data are available in the Supplementary Material.

Atropselective PCB analyses. Atropselective analyses were carried out with extracts from long-term incubations (ie, 5 or 50 μM PCB 132, 120 min at 37°C, 0.5 mg/ml protein, and 0.5 mM NADPH) and extracts from the 30 min incubations described above. Hydroxylated metabolites were analyzed as methylated derivatives after derivatization with diazomethane. Analyses were performed on an Agilent 6890 gas chromatograph equipped with a μECD detector and a CP-Chirasil-Dex CB (CD) (25 m length, 250 μm inner diameter, 0.12 μm film thickness; Agilent, Santa Clara, California) or a ChiralDex G-TA (GTA) capillary column (30 m length, 250 μm inner diameter, 0.12 μm film thickness; Supelco) (Kania-Korwel *et al.*, 2011; Uwimana *et al.*, 2017). The following temperature program was used for the atropselective analysis of PCB 132 and 5′-132 on a CD column: initial temperature was 50°C, hold for 1 min, ramped at 10°C/min to 160°C, hold for 220 min, ramped at 20°C/min to 200°C, and hold for 10 min. To analyze 3′-140 on a GTA column, the temperature program was as follows: initial temperature was 50°C, hold for 1 min, ramped at 10°C/min to 150°C, hold for 400 min, ramped at 10°C/min to 180°C, and hold for 40 min. The helium flow was 3 ml/min for all atropselective analyses. To facilitate a comparison with earlier studies (Kania-Korwel and Lehmler, 2016b; Uwimana *et al.*, 2016, 2017; Wu *et al.*, 2011), enantiomeric fractions (EFs) were calculated by the drop valley method (Asher *et al.*, 2009) as EF = Area E_1/(Area E_1 + Area E_2), with Area E_1 and Area E_2 denoting the peak area of the first (E_1)and second (E_2) eluting atropisomer on the respective column. All EF values are summarized in the Supplementary Table 6.

Quality assurance and quality control. The response of the μECDs used in this study was linear for all analytes up to concentrations of 1000 ng/ml ($R^2 \geq 0.999$). The recoveries of PCB 117 were 93 ± 13% ($n = 120$). Recoveries of 4′-159 could not be determined due to coelution with 4′,5′-132. The limits of detection (LOD) of the PCB 132 metabolites were calculated from blank buffer samples as LOD = mean of blank samples + $k \times$ standard deviation of blank samples, where k is the student's t test value for a degree of freedom $n - 1 = 5$ at 99% confidence level (Kania-Korwel *et al.*, 2011; Uwimana *et al.*, 2016; Wu and Lehmler, 2016; Wu *et al.*, 2011). The LODs were 0.03, 0.1, and 0.21 ng for 3′-140, 5′-132, and 4′-132, respectively. The background levels for 3′-140, 5′-132, and 4′-132 in control (DMSO) incubations with HLMs ($n = 6$) were 0.17, 0.13, and 0.19 ng, respectively. The resolution of the atropisomers of PCB 132 and 5′-132 on the CD column was 1.05 and 2.02, respectively. The resolution of the atropisomers of 3′-140 on the GTA column was 1.18. The EF values of the racemic standards of PCB 132, 3′-140, and 5′-132 were 0.51 ± 0.01 ($n = 2$), 0.50 ± 0.01 ($n = 3$), and 0.49 ± 0.01 ($n = 3$), respectively.

Cell culture. PC12 cells were purchased from American Tissue Culture Collection (Manassas, Virginia) and maintained in RPMI 1640 medium with 10% HS, 5% FBS, and 1% penicillin-streptomycin. Cells were kept in a humidified incubator at 37°C with 5% CO_2 in a 100 mm^2 tissue culture petri dish at a density of 5×10^6 cells. For experiments, cells were plated in 6-well plates in 2 ml medium at a density of 1.5×10^6 cells per well, or in a Collagen I coated 96-well plate at 50.5×10^3 cells per well. N27 cells, a generous gift from Dr Jau-Shyong at the National Institute of Environmental Health Sciences (Research Triangle Park, NC, USA), were maintained in RPMI 1640 with 10% HS, and 1% penicillin-streptomycin. Cells were maintained in a humidified environment at 37°C with 5% CO_2 in a 100 mm^2 collagen-coated tissue culture petri dish at a density of 1×10^6 cells. For experiments, cells were plated in collagen-coated 96-well plates at 5×10^3 cells per well.

Cell viability and production of reactive oxygen species. Cell viability was determined in N27 and PC12 cells using the MTT (3-(4,5-dimethylthiazol-2-yl)-2,5-diphenyltetrazolium bromide) assay (van Meerloo *et al.*, 2011). The formation of reactive oxygen species (ROS) was measured in N27 cells using the DCFDA and dihydroethidium (DHE) fluorescent probes (Chen *et al.*, 2010; Speisky *et al.*, 2009; Zhao *et al.*, 2003). Details regarding these assays are provided in the Supplementary Material.

Dopamine metabolite analysis using HPLC. Intracellular and extracellular dopamine metabolites were measured in PC12 lysate samples via an Agilent 1100 Series capillary HPLC system with an ESA Coulochem III coulometric electrochemical detector (Enayah *et al.*, 2018). After seeding the cells in 6-well plates, they were kept under the same growth conditions for 48 h. Media was then removed and replaced with HEPES buffer (115 mM NaCl, 5.4 mM KCl, 1.8 mM $CaCl_2$, 0.8 mM $MgSO_4$, 5.5 mM glucose, 1 mM NaH_2PO_4, and 15 mM HEPES, pH = 7.4). The cells were then exposed to the PCB 132 atropisomers at 10 and 25 μM and incubated for 24 h at which point cell lysate was collected. After removing the extracellular buffer, 400 μl lysis buffer (10 mM potassium phosphate, 0.1% triton-X, pH = 7.4) was added to each well. Then a cell scraper was used to collect the cell lysate which was stored at −20°C until analysis. On the day of HPLC analysis, the samples were centrifuged at 10 000 g for 10 min, and 3 μl of supernatant injected into the HPLC to measure intracellular dopamine and its metabolites. Separation was achieved with a Phenomenex Synergi C18 column (2 × 150 mm, 80 Å) using an isocratic mobile phase (50 mM citric acid, 1.8 mM sodium heptane sulfonate, 0.2% trifluoroacetic acid, 2% acetonitrile, pH = 3.0) at 200 μl/min. For electrochemical detection of catechol-containing compounds, the following settings were used: guard = + 350, E1 = −150, and E2 = + 200 mV, respectively.

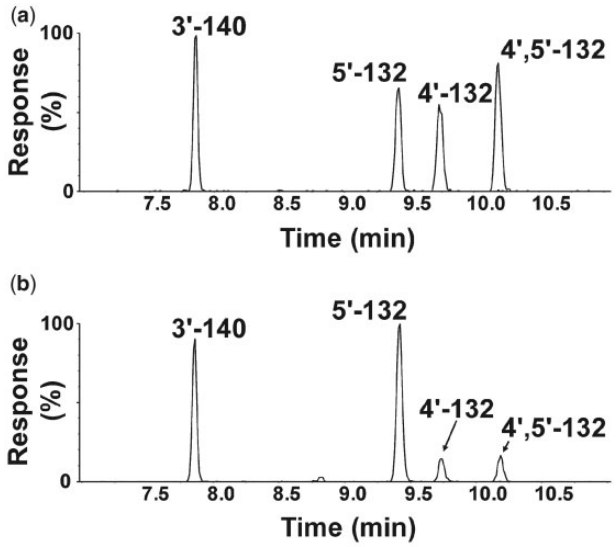

Figure 2. Three monohydroxylated (*m*/*z* 387.9) and 1 dihydroxylated (*m*/*z* 417.9) metabolite were identified in incubations of racemic 2,2′,3,3′,4,6′-hexachlorobiphenyl (PCB 132) with pooled human liver microsomes (pHLMs). Representative gas chromatograms showing (a) the reference standard containing 4 hydroxylated PCB 132 metabolites and (b) an extract from a representative incubation of racemic PCB 132 with pHLMs. All metabolites were analyzed as the corresponding methylated derivatives. Incubations were carried out with 50 μM racemic PCB 132, 0.3 mg/ml microsomal protein, and 1 mM NADPH for 90 min at 37°C (Uwimana *et al.*, 2016, 2018). Analyses were performed by gas chromatography with time-of-flight mass spectrometry (GC-TOF/MS) as described under Materials and Methods. The metabolites were identified based on their retention times relative to the authentic standard and their *m*/*z*. For the corresponding mass spectra, see Supplementary Figures 4–11.

The amount of dopamine, DOPAC, and DOPET was determined by comparison to a standard curve and presented as picomole of analyte per milligram of protein. Details regarding the measurement of dopamine and its metabolites in extracellular media are provided in the Supplementary Material. A bicinchoninic acid assay was used on the PC12 lysate samples as previously described to attain the protein concentration (Walker, 1994).

RESULTS

Identification and Quantification of PCB 132 Metabolites in Incubations With pHLMs

Several human biomonitoring studies have reported an atropisomeric enrichment of PCB 132 in human samples (Supplementary Table 8) (Lehmler *et al.*, 2010); however, the atropselective oxidation of this PCB congener to hydroxylated metabolites by HLMs has not been studied to date (Grimm *et al.*, 2015; Kania-Korwel and Lehmler, 2016a). Our GC-TOF/MS analyses revealed the formation of 3 monohydroxylated and 1 dihydroxylated PCB metabolite in incubations of racemic PCB 132 with pHLMs (Figure 2; Supplementary Figs. 4–11). The structure of these metabolites is shown in the simplified metabolism scheme in Figure 1. Their identification was based on accurate mass determinations, the chlorine isotope patterns of their molecular ion (analyzed as methylated derivatives) and their fragmentation patterns; for additional discussion, see the Supplementary Material. PCB 132 was oxidized by pooled and individual donor HLMs in the *meta* position, with 5′-132 and 3′-140 being major metabolites (Figs 3 and 4; Supplementary Table 2). 3′-140 is a 1,2-shift product (Guroff *et al.*, 1967) that is formed via an arene oxide intermediate, followed by a 1,2-shift of the 3′-chlorine substituent to the *para* position. 4′-132 was only a minor metabolite. 4′,5′-132 could not be quantified in this study due to coelution with the recovery standard, 4′-159; however, this metabolite was only a minor metabolite. PCB 132 was not oxidized in the 2,3,4-chloro substituted ring.

Metabolism of PCB 132 in Comparison to Structurally Related PCBs

As shown in Figure 4a, the PCB 132 metabolite profiles formed by HLMs differs considerably from the profiles of structurally related PCB congeners with a 2,3,6-trichlorophenyl group (ie, PCB 91, PCB 95, and 2,2′,3,3′,6,6′-hexachlorobiphenyl [PCB 136]). HLMs oxidized PCB 132 in the *meta* position to yield the 1,2-shift product, 3′-140, and 5′-132. PCB 91, which is structurally similar to PCB 132, was also primarily metabolized to a 1,2-shift product by HLMs (Uwimana *et al.*, 2018). PCB 95 was preferentially oxidized by HLMs in the *para* position with the lower chlorinated, 2,5-dichloro substituted phenyl ring, and only traces of a 1,2-shift product were formed by different HLM preparations (Uwimana *et al.*, 2016). PCB 136 was metabolized in both the *meta* and *para* position to yield comparable levels of 5′-136 and 4′-136 (Schnellmann *et al.*, 1983; Wu *et al.*, 2014).

To assess if the congener-specific differences in OH-PCB metabolite profiles are due to different arene oxide intermediates or different substitution patterns in the second phenyl ring of chiral PCB congeners, the energetics of the 3,4-arene oxide ring opening reactions were determined for 1,2,4-trichlorobenzene, 2,3,6-trichlorobiphenyl, PCB 91, PCB 95, PCB 132, and PCB 136 (Figure 5; Supplementary Figure 12 and Table 5). Also, complete ring opening pathways were computed for the 3,4-, 4,5-, and 5,6-arene oxides of a single atropisomer of PCB 132 and PCB 136, another environmentally relevant PCB congener (Supplementary Table 5). Because the 3,4-, 4,5-, and 5,6-arene oxides may open in 2 directions, 6 pathways were computed for both PCB 132 and PCB 136.

In the case of the 3,4- and 5,6-arene oxides, the arene oxide opening toward the C–Cl group and the 1,2-shift of the chlorine were concerted, with barriers to the opening of approximately 25 kcal/mol (Supplementary Figure 12). The proton transfer step to form the phenol and restore aromaticity proceeded with a negligible barrier and was essentially spontaneous. Partial pathways opening toward C–Cl were further explored for the 3,4-arene oxides of 1,2,4-trichlorobenzene, 2,3,6-trichlorobiphenyl, PCB 91 and PCB 95. The presence or absence of the substituent aryl ring had no effect on the computed mechanism or energetics for an opening toward C–Cl, nor did the substitution pattern on the aryl substituent.

The energy barrier to arene oxide opening was approximately 40 kcal/mol for both arene oxides when the 3,4- and 5,6-arene oxides open toward the aromatic C–H bond (Figure 5). For both the 3,4- and 5,6-arene oxides, this mode of opening leads to formation of the 4,5-arene oxide as confirmed by IRC calculations, and not the formation of OH-PCB. Because both possible openings of the 4,5-arene oxide also proceed toward C–H, it is not surprising that the barriers for 4,5-arene oxide opening were also approximately 40 kcal/mol. Here, IRC calculations revealed concerted 1,2-hydride shifts analogous to the 1,2-chloride shift observed for 3,4-arene oxide opening toward C–Cl. Overall, the computational results suggest that the formation of 1,2-shift products, such as 3′-140, is energetically favored for all PCB arene oxides investigated.

Interindividual Differences in PCB 132 Metabolism by HLMs

In experiments with single donor HLMs, the formation rates of the monohydroxylated PCB 132 metabolites displayed

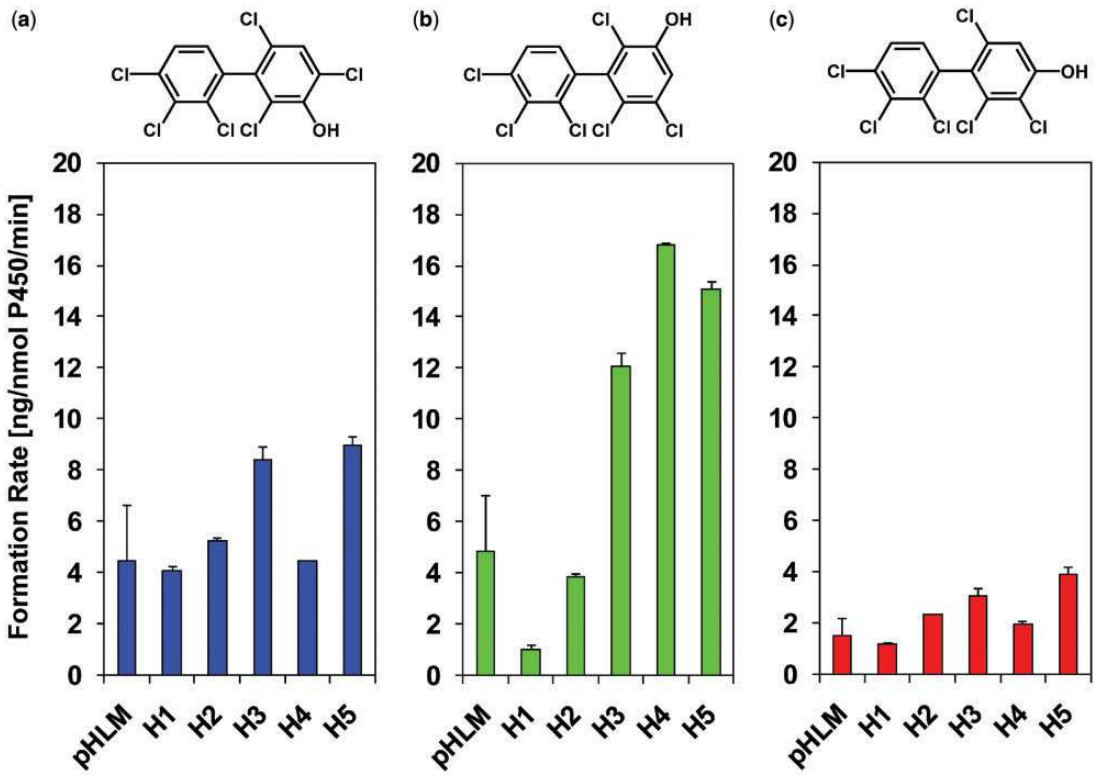

Figure 3. Formation rates of 2,2′,3,3′,4,6′-hexachlorobiphenyl (PCB 132) metabolites by different human liver microsome (HLM) preparations display interindividual differences, with (a) the *meta* hydroxylated metabolites, 2,2′,3,4,4′,6′-hexachlorobiphenyl-3-ol (3′-140; 1,2-shift product), and (b) 2,2′,3,3′,4,6′-hexachlorobiphenyl-5′-ol (5′-132), being major metabolites, and (c) the *para* hydroxylated metabolite, 4′-132, being a minor metabolite. Incubations were carried out with 50 μM racemic PCB 132, 0.1 mg/ml microsomal protein, and 1 mM NADPH for 10 min at 37°C (Supplementary Tables 3 and 4) as reported earlier (Uwimana *et al.*, 2016, 2018). Extracts from the microsomal incubations were derivatized with diazomethane and analyzed by GC-μECD; see Materials and Methods section for additional details. Data are presented as mean ± standard deviation, $n = 3$.

interindividual variation (Figs 3 and 4b; Supplementary Tables 3 and 4). The sum of OH-PCBs (ΣOH-PCBs) formed by single donor HLM preparations followed the following rank order: donor H5 > H4 ~ H3 > H2 ~ pHLM > H1. Notably, levels of ΣOH-PCB were 4.5-fold higher in incubations with HLMs from donors H5 versus H1. The rate of 5′-132 formation differed 16-fold for incubations with HLM preparations from donors H1 versus H4. The rate of 3′-140 and 4′-132 formation differed 2.2- and 3.3-fold, respectively, for incubations with HLM preparations from donors H1 versus H5. As a consequence, the OH-PCB metabolite profiles differed across the HLM preparations investigated (Figure 4b). Briefly, 3′-140 and 5′-132 were formed in a 1:1 ratio by pHLMs. In incubations with HLMs from donors H1 and H2, the 3′-140 to 5′-132 ratios were 3.9:1 and 1.4:1 for donors H1 and H2, respectively. In contrast, 5′-132, and not 3′-140, were major in incubations with HLMs from donors H3, H4, and H5 (3′-140 to 5′-132 ratios were 0.7:1, 0.3:1 and 0.6:1 for donors H3, H4, and H5, respectively). Although only a small number of single donor HLM preparations were investigated in this and other studies, the profiles of OH-PCB metabolite formed in the liver likely display considerable variability in humans.

Atropisomeric Enrichment of PCB 132

Because chiral PCBs undergo atropisomeric enrichment *in vivo* and affect toxic endpoints in an atropselective manner (Kania-Korwel and Lehmler, 2016a; Lehmler *et al.*, 2010), the enrichment of PCB 132 atropisomers in incubations of racemic PCB 132 with HLMs was investigated with atropselective gas chromatography. E_2-PCB 132 (EF = 0.39), which corresponds to (+)-PCB 132 (Haglund and Wiberg, 1996), was enriched in experiments with low PCB 132 concentration (5 μM) and long incubation time (120 min) (Figure 6, Supplementary Table 6). EF values were near racemic in incubations with higher PCB 132 concentrations (50 μM) because the large amount of racemic PCB 132 masked the atropselective depletion of one PCB 132 atropisomer over the other (Uwimana *et al.*, 2016, 2018).

Atropselective Formation of OH-PCB 132 Metabolites

Several studies have reported the atropselective formation of chiral OH-PCB metabolites, both from chiral and prochiral PCBs, in *in vitro* and *in vivo* studies (Kania-Korwel and Lehmler, 2016a; Lehmler *et al.*, 2010; Uwimana *et al.*, 2017). Consistent with these earlier studies, we observed the atropselective formation of different OH-PCB 132 metabolites in incubations with HLMs. Specifically, the atropselective analysis on the GTA column revealed the atropselective formation of E_1-3′-140, with EF values > 0.8 (range: 0.84–0.95) (Figs 6 and 7). E_2-5′-132 was significantly enriched with EF values < 0.2 (range: 0.12–0.18) in incubations with HLMs. As reported previously, the atropisomers of 4′-132 could not be resolved on any of the chiral columns used (Kania-Korwel *et al.*, 2011).

To determine which of E_1-OH-PCB and E_2-OH-PCB atropisomer is formed from (−)- or (+)-PCB 132, we investigated the metabolism of (−)-, (±)-, and (+)-PCB 132 by pHLMs (Figure 8, Supplementary Table 7). The atropselective analysis showed that E_1-5′-132 is formed from (+)-PCB 132. Conversely, E_1-3′-140 and E_2-5′-132 are formed from (−)-PCB 132. The ΣOH-PCBs formed from (−)-PCB 132 was 3-times the ΣOH-PCBs formed

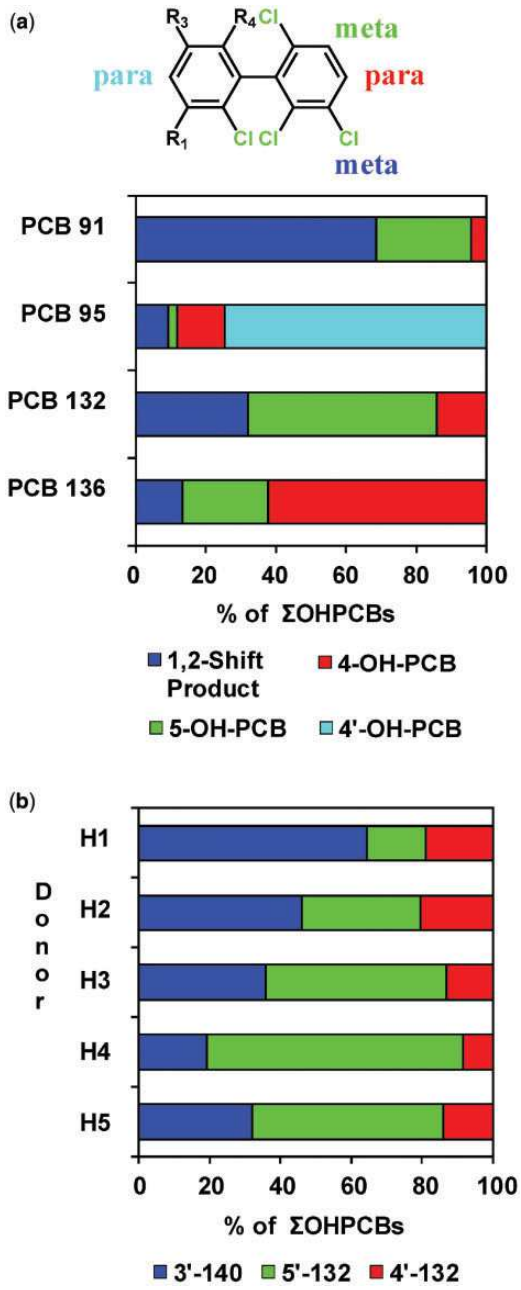

Figure 4. The OH-PCB metabolite profile of 2,2′,3,3′,4,6′-hexachlorobiphenyl (PCB 132) formed by pooled human liver microsomes (pHLMs) is (a) distinctively different from the published metabolite profiles of structurally related PCB congeners (ie, PCB 91, PCB 95, and PCB 136) and (b) shows considerable interindividual variability. a, Bar diagram comparing the profiles of hydroxylated metabolites of PCB 91, PCB 95, PCB 132, and PCB 136 formed in incubations with pHLMs. PCB 91 (Uwimana *et al.*, 2018) and PCB 132 (this study) are preferentially oxidized in *meta* position, including the formation of 1,2-shift products, whereas PCB 95 (Uwimana *et al.*, 2016) and PCB 136 (Wu *et al.*, 2014) are hydroxylated in *para* position. In the case of PCB 95, the oxidation occurs preferentially in the *para* position of the lower chlorinated 2,5-dichlorophenyl ring (Uwimana *et al.*, 2016). Incubations were carried out with 50 μM PCB, 0.1 mg/ml microsomal protein, and 1 mM NADPH for 5 min (PCB 91 and PCB 95) or 10 min (PCB 132 and PCB 136) at 37°C using the same pHLM preparation. b, Bar diagram showing interindividual differences in profiles of hydroxylated metabolites of PCB 132 formed in incubations with different single donor human liver microsome (HLM) preparations. Incubations were carried out with 50 μM PCB 132, 0.1 mg/ml microsomal protein and 1 mM NADPH for 10 min at 37°C (Uwimana *et al.*, 2016, 2018). Extracts from the microsomal incubations were derivatized with diazomethane and analyzed by GC-μECD; see Materials and Methods section for additional details.

from (+)-PCB 132 (Supplementary Table 7). A more complex picture emerges when individual OH-PCB 132 metabolites are analyzed (Figs. 8e–g). The levels of both major metabolites, 3′-140 and 5′-132, decreased in the order of (−)-PCB 132 > (±)-PCB 132 > (+)-PCB 132. In contrast, levels of the minor metabolite, 4′-132, decreased in the reverse order. As a consequence, the OH-PCB 132 metabolite profiles formed by HLMs differ considerably for incubations with (−)-, (±)-, and (+)-PCB 132 (Figure 8h).

Cytotoxicity and Oxidative Stress of PCB 132 Atropisomers

It is currently unknown if pure PCB atropisomers differentially cause cytotoxicity or atropselectively increase the production of ROS in dopaminergic cells. In our study, PCB 132 atropisomers did not elicit overt cytotoxicity in immortalized dopaminergic cell lines as determined by MTT analysis (Supplementary Figure 13). Both (+)-PCB 132 and (−)-PCB 132 exerted measurable toxicity to N27 cells only at the highest dose (100 μM) with a 24 h exposure. Analogously, PC12 cells showed no significant cell loss following PCB 132 atropisomer exposure. We observed a slight increase in overall ROS and hydrogen peroxide, measured with DCFDA and DHE, respectively, after 24 h exposure of N27 cells to PCB 132 atropisomers; however, these changes did not reach statistical significance (Supplementary Figure 14). Similarly, no statistically significant, time-dependent changes in the production of ROS were observed at earlier time intervals (data not shown). There were also no significant differences in the effects of both PCB 132 atropisomers on dopaminergic cellular toxicity and levels of ROS.

Effect of PCB 132 on Levels of Dopamine and Its Metabolites

PCBs, including chiral PCB 95, have been shown to affect the dopaminergic system, including by altering the expression of dopamine receptors and by changing dopamine levels (Bavithra *et al.*, 2012; Enayah *et al.*, 2018; Seegal *et al.*, 2002); however, it is unknown if PCBs atropselectively affect the dopaminergic system and dopamine metabolism. PC12 cells were exposed to PCB atropisomers for 24 h, and intracellular dopamine and its metabolites were measured via HPLC analysis. Dopamine is converted by monoamine oxidase to DOPAL which is further metabolized by aldehyde dehydrogenase to DOPAC or by aldehyde reductase to DOPET. Intracellular levels of dopamine, DOPAC, and DOPET showed no significant differences from control (Figure 9). Extracellular levels of dopamine and DOPAC was also measured in media with similar results (Supplementary Figure 15).

DISCUSSION

PCB 132 is readily metabolized by HLMs to a 1,2-shift product, 3′-140, and a second *meta* hydroxylated metabolite, 5′-132. Several structurally related PCB congeners with multiple *ortho* chlorine substituents are also metabolized by HLMs to OH-PCBs (Nagayoshi *et al.*, 2018; Schnellmann *et al.*, 1983; Wu *et al.*, 2014). For example, PCB 91 is primarily metabolized to a 1,2-shift product by HLMs (Uwimana *et al.*, 2018), whereas PCB 95 and PCB 136 are oxidized by HLMs with different regioselectivity (Schnellmann *et al.*, 1983; Uwimana *et al.*, 2016; Wu *et al.*, 2014). Based on published structure-metabolism relationships (Grimm *et al.*, 2015), these congener-specific differences in their metabolism are likely due to the presence of a *para* chlorine substituent in PCB 91 and PCB 132, but not PCB 95 and PCB 136. The formation of a 1,2-shift product indicates that similar to PCB 91, PCB 132 is oxidized by human P450 enzymes to an arene oxide

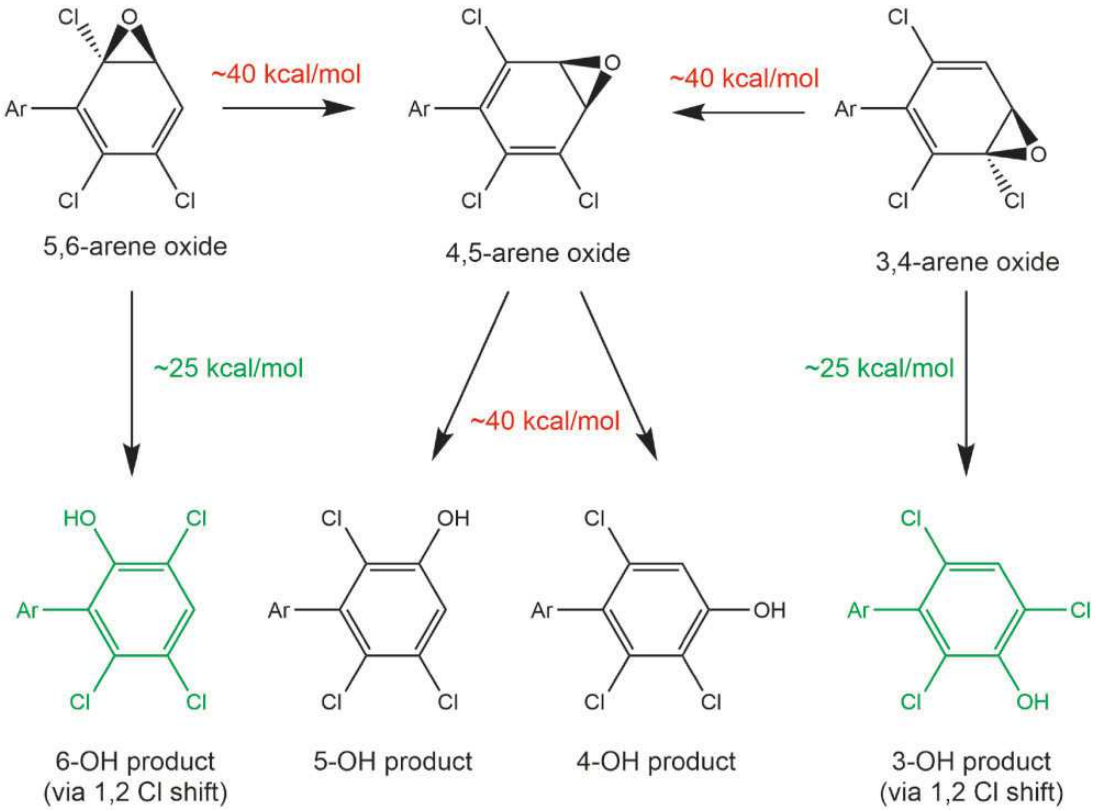

Figure 5. The formation of 1,2-chlorine shift metabolites via arene oxide intermediates of chiral polychlorinated biphenyls (PCBs) is energetically favored. Energies shown are free energies of activation at the M11/def2-SVP level of theory with the SMD aqueous continuum solvation model. Abbreviations: Ar—2′,4′-dichlorophenyl for PCB 91; PCB 95—2′,5′-dichlorophenyl; PCB 132—2,3,4-trichlorophenyl; PCB 136—2′,3′,6′-dichlorophenyl.

intermediate that subsequently undergoes a 1,2-chlorine shift to 3′-140. Importantly, different OH-PCB profiles have been reported for the metabolism of these PCB congeners in rodent models used to study the neurotoxicity of PCBs (Kania-Korwel *et al.*, 2017; Schantz *et al.*, 1997; Wayman *et al.*, 2012). For example, 5′-132, and not 3′-140, was the major metabolite formed from PCB 132 in experiments with rat liver microsomes (Kania-Korwel *et al.*, 2011), recombinant rat CYP2B1 (Lu *et al.*, 2013), and precision-cut mouse liver tissue slices (Wu *et al.*, 2013a). 1,2-Shift products were only minor metabolites of PCB 132 and other chiral PCBs in *in vitro* and *in vivo* studies in rodent models (Kania-Korwel *et al.*, 2011; Lu *et al.*, 2013; Wu *et al.*, 2013a).

The preferential formation of different PCB arene oxide intermediates in rodents versus humans is one explanation for the species differences in the oxidation of PCB 132 and structurally related PCB congeners. We employed a computational approach to study the energetics of the ring opening of the 3 possible arene oxides on the 2,3,6-trichloro-substituted phenyl ring to explore this possibility. Independent of the position of the arene oxide, our calculations suggested that (1) the ring opening leading to a 1,2-shift of chlorine substituents is energetically favorable over a ring opening toward C–H and (2) the presence of the second aromatic ring does not perturb the energetics of the arene oxide ring opening. Based on our computational results, the 1,2-shift products of PCB 132 (this study) and PCB 91 (Uwimana *et al.*, 2018) are formed via a 3,4-arene oxide intermediate which opens toward C–Cl to form the 1,2-shift metabolite. The presence or absence of the substituent aryl ring had no effect on the computed mechanism or energetics for an opening toward C–Cl, nor did the substitution pattern on the aryl substituent. This is expected given the lack of conjugation between the 2 aryl rings due to their (near) orthogonality. The computational results therefore suggest that the formation of *para*-substituted metabolites of PCB 95 and PCB 136 is not merely due to the energetically favored opening of the 3,4- or 4,5-arene oxide intermediates. Instead, congener-specific differences in the steric or electronic interaction of both PCB congeners with P450 isoforms involved in their metabolism (Uwimana *et al.*, 2019) likely affect the ring opening of the putative arene oxide intermediates to OH-PCBs. In contrast, the formation of OH-PCB metabolites of PCB 132 and related PCB congeners in rodents may or may not involve an arene oxide intermediate. For example, the *meta* oxidation of PCB 52 by rat CYP2B1 does not involve an arene oxide but occurs via the insertion of an oxygen atom into the aromatic C–H bond (Preston *et al.*, 1983). Other PCB congeners are readily metabolized via arene oxide intermediates by P450 enzymes (Kennedy *et al.*, 1981; Schnellmann *et al.*, 1983).

In addition to congener and species-dependent differences in the OH-PCB metabolite profiles, we observed considerable interindividual variability in the formation of PCB 132 metabolites by HLM preparations from different donors. For example, differences as high as 16-fold were found in the formation of 5′-132 by different HLM preparations. Similarly, we reported interindividual differences in the formation of OH-PCB metabolites of PCB 91 and PCB 95 with the same HLM preparations (Uwimana *et al.*, 2016, 2018). This observation is not surprising considering the well-documented variability of P450 enzyme activities among humans (Guengerich, 2015). As we reported recently, both CYP2A6 and CYP2B6 are involved in the

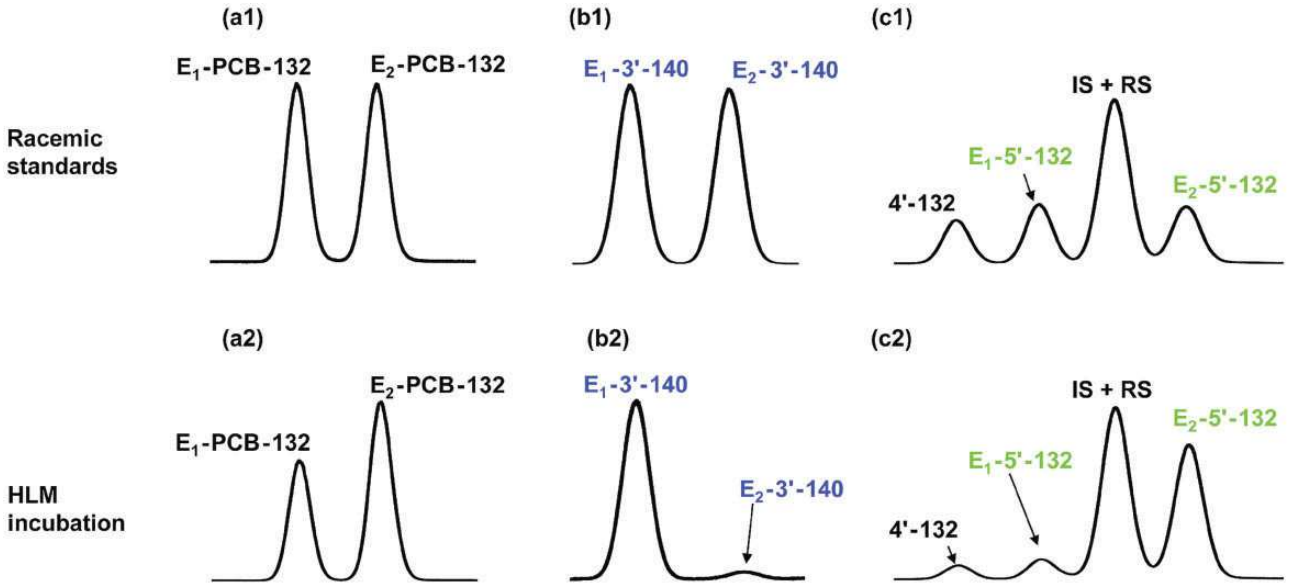

Figure 6. Atropselective gas chromatographic analysis revealed the atropselective metabolism of racemic 2,2′,3,3′,4,6′-hexachlorobiphenyl (PCB 132) to 2,2′,3,3′,4,6′-hexachlorobiphenyl-5′-ol (5′-132) and 2,2′,3,4,4′,6′-hexachlorobiphenyl-3-ol (3′-140) in incubations with pooled human liver microsomes (pHLMs). Representative gas chromatograms of racemic standards (top panels) versus PCB 132, 5′-132, and 3′-140 in incubations of racemic PCB 132 with human liver microsomes (HLMs) (bottom panels) show a depletion of E_1-PCB 132 (panels a1 vs a2) and atropselective formation of E_1-3′-140 (panels b1 vs b2) and E_2-5′-132 (panels c1 vs c2). To assess the atropselective depletion of PCB 132, incubations were carried out with 5 μM PCB 132, 0.5 mg/ml microsomal protein (pHLMs only), and 0.5 mM NADPH for 120 min at 37°C. To study the atropselective formation of the PCB 132 metabolites, incubations were carried out with 50 μM racemic PCB 132, 0.1 mg/ml microsomal protein, and 1 mM NADPH for 30 min at 37°C (donor H3 shown here; see Figure 7 for results from incubations using other HLM preparations) (Uwimana *et al.*, 2016, 2018). Metabolites were analyzed as the corresponding methylated derivatives after derivatization with diazomethane. Atropselective analyses of 3′-140 were performed with a ChiralDex G-TA (GTA) column at 150°C, and atropselective analyses of PCB 132 and 5′-132 were carried out with a CP-Chirasil-Dex CB (CD) column at 160°C (Kania-Korwel *et al.*, 2011).

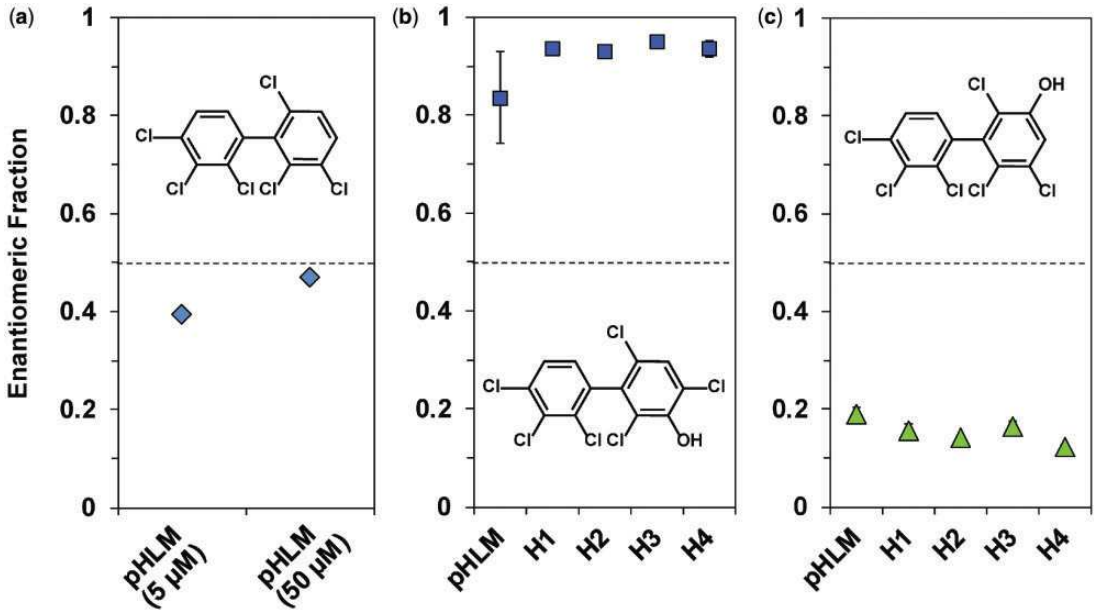

Figure 7. Enantiomeric fractions (EFs) of (a) parent 2,2′,3,3′,4,6′-hexachlorobiphenyl (PCB 132), (b) 2,2′,3,4,4′,6′-hexachlorobiphenyl-3-ol (3′-140), and (c) 2,2′,3,3′,4,6′-hexachlorobiphenyl-5′-ol (5′-132) reveal only small interindividual differences in the atropselective formation of both OH-PCB metabolites. a, To assess the atropselective depletion of PCB 132, incubations were carried out with 5 μM or 50 μM PCB 132, 0.5 mg/ml microsomal protein (using pooled human liver microsomes [pHLMs] only), 0.5 mM NADPH for 120 min at 37°C (see Figure 6 for a representative chromatogram). To study the atropselective formation of (b) 3′-140 and (c) 5′-132, microsomal incubations were carried out with 50 μM racemic PCB 132, 0.1 mg/ml microsomal protein, 1 mM NADPH for 30 min at 37°C (Uwimana *et al.*, 2016, 2018). Metabolites were analyzed as the corresponding methylated derivatives. Atropselective analyses of 3′-140 were performed with a ChiralDex G-TA (GTA) column at 150°C, and atropselective analyses of PCB 132 and 5′-132 were carried out with a CP-Chirasil-Dex CB (CD) column at 160°C (Kania-Korwel *et al.*, 2011). EF values could not be determined in incubations with human liver microsomes (HLMs) from donor H5 due to the low metabolite levels. Data are presented as mean ± standard deviation, $n = 3$. The dotted line indicates the EF values of the racemic standards.

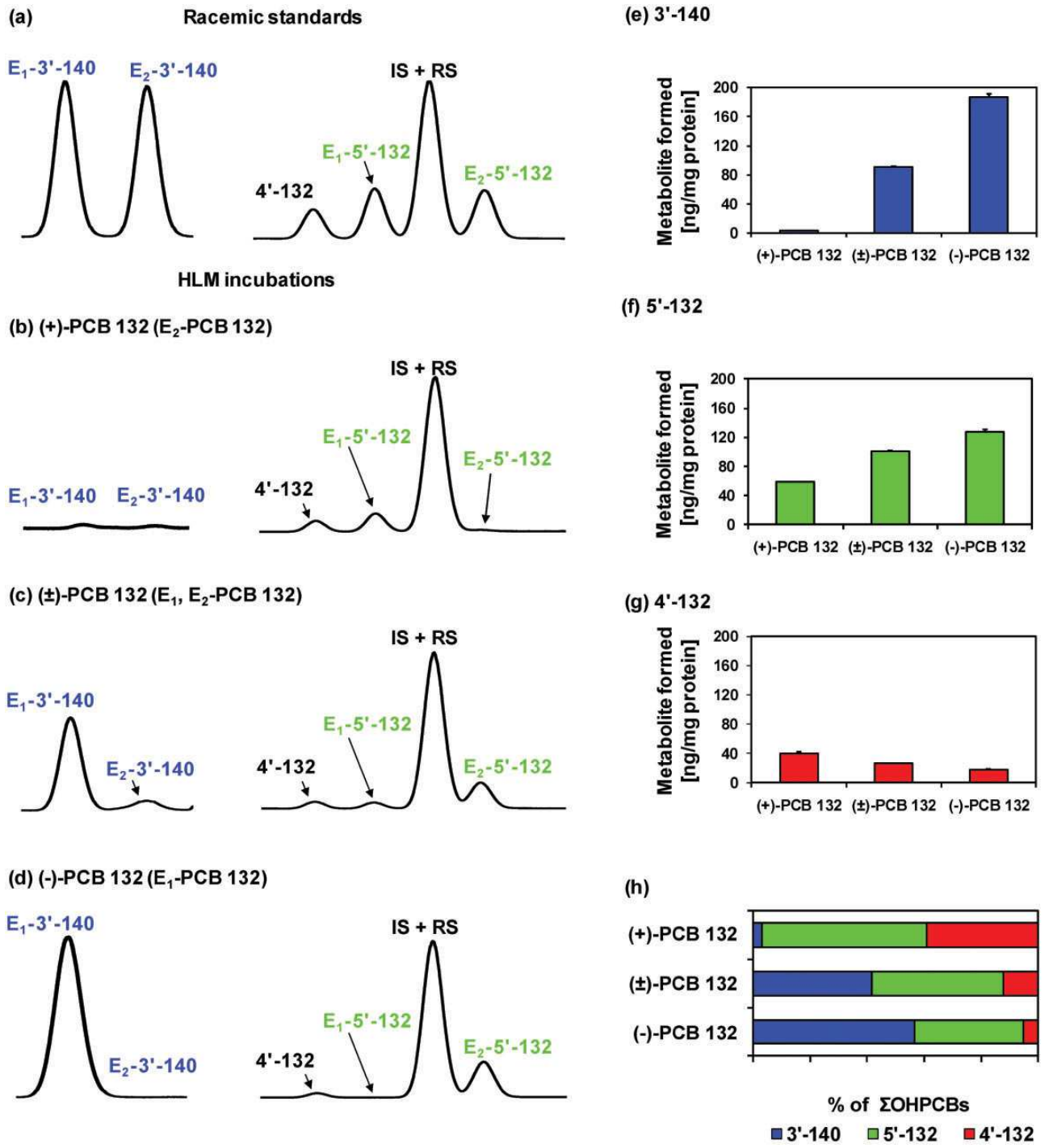

Figure 8. Comparison of representative gas chromatograms of (a) racemic OH-PCB metabolite standards with OH-PCB metabolites formed in incubations of (b) (+)-PCB 132 (2,2′,3,3′,4,6′-hexachlorobiphenyl), (c) (±)-PCB 132, or (d) (−)-PCB 132 with pooled human liver microsomes (pHLMs) reveals that E_1-5′-132 (2,2′,3,3′,4,6′-hexachlorobiphenyl-5′-ol) is formed from (+)-PCB 132 and E_1-3′-140 (2,2′,3,4,4′,6′-hexachlorobiphenyl-3-ol), and E_2-5′-132 are formed from (−)-PCB. Moreover, (e) 3′-140 and (f) 5′-132, but not (g) 2,2′,3,3′,4,6′-hexachlorobiphenyl-4′-ol (4′-132) are formed more rapidly from (−)-PCB 132 than (+)-PCB 132, resulting (h) in distinct OH-PCB metabolite profiles formed from (+)-, (±)-, and (−)-PCB 132 in incubations with pHLMs. Incubations were carried out with 50 μM (+)-PCB 132, racemic PCB 132, or (−)-PCB 132, 0.1 mg/ml microsomal protein and 1 mM NADPH for 30 min at 37°C (Uwimana *et al.*, 2016). Metabolites were analyzed as the corresponding methylated derivatives after derivatization with diazomethane. Atropselective analyses of 3′-140 were performed with a ChiralDex G-TA (GTA) column at 150°C, and atropselective analyses of PCB 132 and 5′-132 were carried out with a CP-Chirasil-Dex CB (CD) column at 160°C. 4′-132 was not resolved on any of the columns used in this study (Kania-Korwel *et al.*, 2011). Data are presented as mean ± standard deviation, $n = 3$.

metabolism of PCB 132 (Uwimana *et al.*, 2019). CYP2A6 primarily formed 3′-140, with 5′-132 and 4′-132 being minor metabolites. CYP2B6 primarily yielded 5′-132, with the 1,2-shift product being a minor metabolite. Differences in the levels of CYP2A6 and CYP2B6 in the HLM preparations investigated are one explanation for the interindividual differences in the OH-PCB formation rates in this and our earlier studies. Moreover, both CYP2A6 and CYP2B6 are highly polymorphic enzymes (PharmWar, 2012,

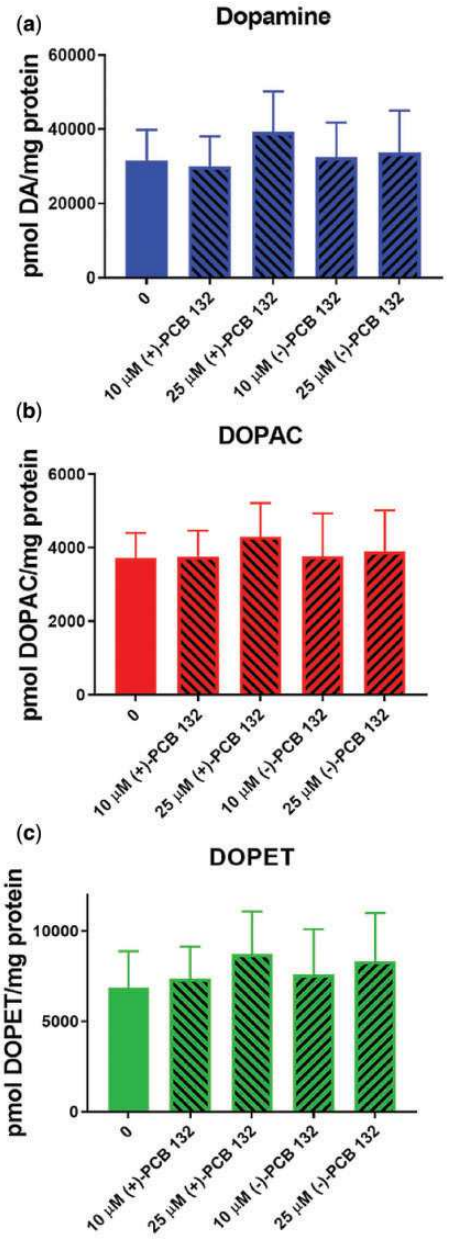

Figure 9. Exposure of PC12 cells for 24 h to (+)- or (−)-PCB 132 (2,2′,3,3′,4,6′-hexachlorobiphenyl) did not significantly alter intracellular levels of (a) dopamine, (b) 3,4-dihydroxyphenylacetic acid (DOPAC), or (c) 3,4-dihydroxyphenyl ethanol (DOPET). Intracellular measurements of dopamine and its metabolites were performed by HPLC analysis with electrochemical detection. Data are represented as mean ± standard error, $n = 4$.

2013). As has been shown for active site mutants of CYP2B1 (Waller *et al.*, 1999), the rat ortholog of CYP2B6, polymorphisms can alter the regioselectivity of the oxidation of PCBs.

The biotransformation of PCB 132 by P450 enzymes results in nonracemic chiral signatures of both the parent PCB and its metabolites in environmental samples and mammals, including humans (Kania-Korwel and Lehmler, 2016b; Lehmler *et al.*, 2010). Importantly, the enrichment of PCB atropisomers observed in *in vitro* studies typically predicts the atropisomeric enrichment in animal studies. (+)-PCB 132 was enriched in *in vitro* metabolism studies with precision-cut mouse liver tissue slices (Wu *et al.*, 2013a), rat liver microsomes (Kania-Korwel *et al.*, 2011), and recombinant rat CYP2B1 and human CYP2B6 (Lu *et al.*, 2013; Warner *et al.*, 2009). Consistent with these *in vitro* metabolism studies, (+)-PCB 132 was enriched in female mice (Kania-Korwel *et al.*, 2010; Milanowski *et al.*, 2010) and male Wistar rats (Norstrom *et al.*, 2006). (−)-PCB 132 had a shorter half-life in a disposition study in mice (Kania-Korwel *et al.*, 2010). In rats, levels of methyl sulfone metabolites of PCB 132 were higher in (−)-PCB 132 compared (+)-PCB 132 exposed animals, suggesting that (−)-PCB 132 is more rapidly metabolized in rats (Norstrom *et al.*, 2006). Analogous to the laboratory studies, the preferential oxidation of (−)-PCB 132 by HLMs observed in this study is consistent with the enrichment of (+)-PCB 132 found in most human samples (Supplementary Table 8). However, other factors may also contribute to the atropisomeric enrichment of PCB 132 in humans. For example, we cannot dismiss the possibility that exposure to atropisomerically enriched PCB 132 via the diet also contributes to the atropisomeric enrichment of PCB 132 in humans (Harrad *et al.*, 2006; Vetter, 2016). More in-depth studies are therefore needed to characterize which P450 isoforms contribute to the atropselective metabolism of PCB 132, and to determine whether or not genetic polymorphisms affect the stereoselectivity of its oxidation.

In addition to the parent PCB, and consistent with earlier studies reporting the atropselective formation of chiral OH-PCB metabolites from PCBs (Kania-Korwel and Lehmler, 2016a; Lehmler *et al.*, 2010; Uwimana *et al.*, 2017), we observed the atropselective formation of OH-PCB 132 metabolites in incubations with HLMs. Specifically, we noted the atropselective formation of E_1-3′-140. This 3′-140 atropisomer was also enriched in experiments with rat liver microsomes (Kania-Korwel *et al.*, 2011). E_2-5′-132 was significantly enriched in incubations with HLMs. Similarly, metabolism of racemic PCB 132 resulted in an enrichment of E_2-5′-132 in incubations with rat liver microsomes (Kania-Korwel *et al.*, 2011) and mouse liver tissue slices (Wu *et al.*, 2013a). In contrast, rat CYP2B1 metabolized PCB 132 preferentially to E_1-5′-132, which indicates the involvement of other P450 isoforms in the atropselective oxidation of PCB 132 in incubations with rat liver microsomes (Lu *et al.*, 2013). The atropselective formation of OH-PCBs by HLMs is important in the context of several findings from laboratory studies: Chiral OH-PCBs present in the developing brain of mice exposed developmentally to racemic PCBs (Kania-Korwel *et al.*, 2017). Moreover, the position of the OH-group has a profound effect on the interaction of OH-PCBs with cellular targets implicated in PCB neurotoxicity (Kodavanti *et al.*, 2003; Niknam *et al.*, 2013). It is therefore likely that interindividual differences in (1) PCB and OH-PCB levels and (2) chiral signatures influence toxic outcomes in humans.

Several studies have shown that PCB atropisomers atropselectively affect endpoints relevant to PCB neurotoxicity, including altered calcium homeostasis, estrogen receptor activation, and ROS, linked to PCB developmental neurotoxicity (Chai *et al.*, 2016; Feng *et al.*, 2017; Lehmler *et al.*, 2005; Pěnčíková *et al.*, 2018; Yang *et al.*, 2014). In our preliminary assessment of the effects of PCB 132 atropisomers on endpoints implicated in PCB neurotoxicity, we saw increased general ROS levels, which are known to damage lipids and proteins, at subtoxic PCB 132 concentrations in dopaminergic cells in culture; however, this effect did not reach statistical significance at the PCB 132 concentrations investigated using cultured dopaminergic cell lines. Toxicity for 2 dopaminergic cell lines was only observed at the highest concentration used (ie, 100 μM). These findings suggest that the PCB 132 atropisomers are not toxic over the periods examined (ie, 4 and 24 h) to yield alterations in dopamine metabolism, cell loss

or increased oxidative stress. Exposure of rats to a PCB mixture containing racemic PCB 132 for 4 weeks leads to changes in levels of dopamine and increased oxidative damage and loss of cells in dopaminergic regions (Lee *et al.*, 2012); therefore, it is possible that more time or PCB 132 metabolism (eg, hydroxylated metabolites) are required before toxicity to dopaminergic systems is apparent (Kodavanti *et al.*, 2003; Niknam *et al.*, 2013). Future work should address these issues.

In addition, it is conceivable that PCB 132 lacks the structural requirements for neurotoxicity. A detailed structure-activity investigation in the same cell line (ie, PC12) showed that PCB congeners with *ortho* substituents result in a decrease in intracellular, total dopamine levels, but that chlorine substituents in *meta* position counteract this effect. The lack of an effect of PCB 132, which contains a *meta* chlorine substituent in both phenyl rings, on cellular dopamine metabolism is therefore not entirely surprising. It is noteworthy that exposure of PC12 cells to racemic PCB 95 decreases dopamine concentrations and increases levels of toxic dopamine metabolites (Enayah *et al.*, 2018). A systematic study of other PCB atropisomers is therefore warranted to assess if PCBs atropselectively cause oxidative stress and alter dopamine homeostasis in the brain and, ultimately, if the atropselective metabolism of PCBs plays a currently unexplored role in PCB-mediated neurotoxicity.

SUPPLEMENTARY DATA

Supplementary data are available at *Toxicological Sciences* online.

DECLARATION OF CONFLICTING INTERESTS

The authors declared no potential conflicts of interest with respect to the research, authorship, and/or publication of this article.

ACKNOWLEDGMENTS

We thank Dr S. Joshi, Dr S. Vyas, and Dr Y. Song (University of Iowa) for synthesizing the PCB standards and Mr V. Parcel from the University of Iowa HRMS Facility for help with the GC-TOF/MS analyses.

FUNDING

This work was supported by the National Institute of Environmental Health Sciences/National Institutes of Health (ES05605, ES013661, and ES027169 to H.L.J., ES029035 to J.A.D.); and the National Science Foundation (CHE-1609669, CHE-1229354 to the MERCURY consortium [http://mercury-consortium.org/ Accessed July 7, 2019], CHE-1662030 to E.V.P.). The content of the manuscript is solely the responsibility of the authors and does not necessarily represent the official views of the National Institute of Environmental Health Sciences, the National Institutes of Health or the National Science Foundation.

REFERENCES

Anderson, D. G., Mariappan, S. V., Buettner, G. R., and Doorn, J. A. (2011). Oxidation of 3,4-dihydroxyphenylacetaldehyde, a toxic dopaminergic metabolite, to a semiquinone radical and an ortho-quinone. *J. Biol. Chem.* **286**, 26978–26986.

Asher, B. J., D'Agostino, L. A., Way, J. D., Wong, C. S., and Harynuk, J. J. (2009). Comparison of peak integration methods for the determination of enantiomeric fraction in environmental samples. *Chemosphere* **75**, 1042–1048.

Bavithra, S., Selvakumar, K., Pratheepa Kumari, R., Krishnamoorthy, G., Venkataraman, P., and Arunakaran, J. (2012). Polychlorinated biphenyl (PCBs)-induced oxidative stress plays a critical role on cerebellar dopaminergic receptor expression: Ameliorative role of quercetin. *Neurotox. Res.* **21**, 149–159.

Bemis, J. C., and Seegal, R. F. (2004). PCB-induced inhibition of the vesicular monoamine transporter predicts reductions in synaptosomal dopamine content. *Toxicol. Sci.* **80**, 288–295.

Bordajandi, L. R., Abad, E., and Gonzalez, M. J. (2008). Occurrence of PCBs, PCDD/Fs, PBDEs and DDTs in spanish breast milk: Enantiomeric fraction of chiral PCBs. *Chemosphere* **70**, 567–575.

Bucheli, T. D., and Brandli, R. C. (2006). Two-dimensional gas chromatography coupled to triple quadrupole mass spectrometry for the unambiguous determination of atropisomeric polychlorinated biphenyls in environmental samples. *J. Chromatogr. A* **1110**, 156–164.

Caudle, W. M., Richardson, J. R., Delea, K. C., Guillot, T. S., Wang, M., Pennell, K. D., and Miller, G. W. (2006). Polychlorinated biphenyl-induced reduction of dopamine transporter expression as a precursor to Parkinson's disease-associated dopamine toxicity. *Toxicol. Sci.* **92**, 490–499.

Chai, T., Cui, F., Mu, X., Yang, Y., Qi, S., Zhu, L., Wang, C., and Qiu, J. (2016). Stereoselective induction by 2,2′,3,4′,6-pentachlorobiphenyl in adult zebrafish (*Danio rerio*): Implication of chirality in oxidative stress and bioaccumulation. *Environ. Pollut.* **215**, 66–76.

Chen, X., Zhong, Z., Xu, Z., Chen, L., and Wang, Y. (2010). 2′,7′-dichlorodihydrofluorescein as a fluorescent probe for reactive oxygen species measurement: Forty years of application and controversy. *Free Radic. Res.* **44**, 587–604.

Chu, S., Covaci, A., and Schepens, P. (2003). Levels and chiral signatures of persistent organochlorine pollutants in human tissues from Belgium. *Environ. Res.* **93**, 167–176.

CYP2A6 pharmacogene variation consortium (pharmvar) at www.Pharmvar.Org. 2012. Available at: https://www.pharmvar.org/gene/CYP2A6. Accessed February 28, 2019.

CYP2B6 pharmacogene variation consortium (pharmvar) at www.Pharmvar.Org. 2013. Available at: https://www.pharmvar.org/gene/CYP2B6. Accessed February 28, 2019.

DeCaprio, A. P., Johnson, G. W., Tarbell, A. M., Carpenter, D. O., Chiarenzelli, J. R., Morse, G. S., Santiago-Rivera, A. L., Schymura, M. J, and Akwesasne Task Force on the Environment. (2005). Polychlorinated biphenyl (PCB) exposure assessment by multivariate statistical analysis of serum congener profiles in an adult native american population. *Environ. Res.* **98**, 284–302.

Enayah, S. H., Vanle, B. C., Fuortes, L. J., Doorn, J. A., and Ludewig, G. (2018). PCB95 and PCB153 change dopamine levels and turn-over in PC12 cells. *Toxicology* **394**, 93–101.

European Commission. (2002). Commission decision EC 2002/657 of 12 August 2002 implementing council directive 96/23/ec concerning the performance of analytical methods and the interpretation of results. *Off. J. Eur Communities* **221**, 0008–0036.

Fellman, J. H. (1958). The rearrangement of epinephrine. *Nature* **182**, 311–312.

Feng, W., Zheng, J., Robin, G., Dong, Y., Ichikawa, M., Inoue, Y., Mori, T., Nakano, T., and Pessah, I. N. (2017).

Enantioselectivity of 2,2′,3,5′,6-pentachlorobiphenyl (PCB 95) atropisomers toward ryanodine receptors (RyRs) and their influences on hippocampal neuronal networks. *Environ. Sci. Technol.* **51**, 14406–14416.

Forgue, S. T., and Allen, J. R. (1982). Identification of an arene oxide metabolite of 2,2′,5,5′-tetrachlorobiphenyl by gas chromatography-mass spectroscopy. *Chem. Biol. Interact.* **40**, 233–245.

Forgue, S. T., Preston, B. D., Hargraves, W. A., Reich, I. L., and Allen, J. R. (1979). Direct evidence that an arene oxide is a metabolic intermediate of 2,2′,5,5′-tetrachlorobiphenyl. *Biochem. Biophys. Res. Commun.* **91**, 475–483.

Frisch, M., Trucks, G., Schlegel, H., Scuseria, G., Robb, M., Cheeseman, J., Scalmani, G., Barone, V., Petersson, G., Nakatsuji, H., *et al.* 2016. *Gaussian 16, Revision a. 03*. Gaussian Inc, Wallingford, CT.

Glausch, A., Hahn, J., and Schurig, V. (1995). Enantioselective determination of chiral 2,2′,3,3′,4,6′-hexachlorobiphenyl (PCB 132) in human milk samples by multidimensional gas chromatography/electron capture detection and by mass spectrometry. *Chemosphere* **30**, 2079–2085.

Grimm, F. A., Hu, D., Kania-Korwel, I., Lehmler, H. J., Ludewig, G., Hornbuckle, K. C., Duffel, M. W., Bergman, A., and Robertson, L. W. (2015). Metabolism and metabolites of polychlorinated biphenyls. *Crit. Rev. Toxicol.* **45**, 245–272.

Guengerich, F. P. 2015. Human cytochrome P450 enzymes. In *Cytochrome P450* (P. R. Ortiz de Montellano, Ed.), pp. 523–785. Springer US, Boston, MA.

Guroff, G., Daly, J. W., Jerina, D. M., Renson, J., Witkop, B., and Udenfriend, S. (1967). Hydroxylation-induced migration: The NIH shift. Recent experiments reveal an unexpected and general result of enzymatic hydroxylation of aromatic compounds. *Science* **157**, 1524–1530.

Haglund, P., and Wiberg, K. (1996). Determination of the gas chromatographic elution sequences of the (+) and (−) enantiomers of stable enantiomeric PCBs on Chirasil-Dex. *J. High Resolut. Chromatogr.* **19**, 373–376.

Haijima, A., Lesmana, R., Shimokawa, N., Amano, I., Takatsuru, Y., and Koibuchi, N. (2017). Differential neurotoxic effects of in utero and lactational exposure to hydroxylated polychlorinated biphenyl (OH-PCB 106) on spontaneous locomotor activity and motor coordination in young adult male mice. *J. Toxicol. Sci.* **42**, 407–416.

Haraguchi, K., Koga, N., and Kato, Y. (2005). Comparative metabolism of polychlorinated biphenyls and tissue distribution of persistent metabolites in rats, hamsters, and guinea pigs. *Drug Metab. Dispos.* **33**, 373–380.

Haraguchi, K., Kato, Y., Koga, N., and Degawa, M. (2004). Metabolism of polychlorinated biphenyls by Gunn rats: Identification and serum retention of catechol metabolites. *Chem. Res. Toxicol.* **17**, 1684–1691.

Harrad, S., Ren, J., Hazrati, S., and Robson, M. (2006). Chiral signatures of PCB#s 95 and 149 in indoor air, grass, duplicate diets and human faeces. *Chemosphere* **63**, 1368–1376.

Hatcher-Martin, J. M., Gearing, M., Steenland, K., Levey, A. I., Miller, G. W., and Pennell, K. D. (2012). Association between polychlorinated biphenyls and Parkinson's disease neuropathology. *Neurotoxicology* **33**, 1298–1304.

Herrick, R. F., Stewart, J. H., and Allen, J. G. (2016). Review of PCBs in US schools: A brief history, an estimate of the number of impacted schools, and an approach for evaluating indoor air samples. *Environ. Sci. Pollut. Res. Int.* **23**, 1975–1985.

Jinsmaa, Y., Florang, V. R., Rees, J. N., Anderson, D. G., Strack, S., and Doorn, J. A. (2009). Products of oxidative stress inhibit aldehyde oxidation and reduction pathways in dopamine catabolism yielding elevated levels of a reactive intermediate. *Chem. Res. Toxicol.* **22**, 835–841.

Jones, D. C., and Miller, G. W. (2008). The effects of environmental neurotoxicants on the dopaminergic system: A possible role in drug addiction. *Biochem. Pharmacol.* **76**, 569–581.

Jursa, S., Chovancova, J., Petrik, J., and Loksa, J. (2006). Dioxin-like and non-dioxin-like PCBs in human serum of Slovak population. *Chemosphere* **64**, 686–691.

Kania-Korwel, I., Duffel, M. W., and Lehmler, H. J. (2011). Gas chromatographic analysis with chiral cyclodextrin phases reveals the enantioselective formation of hydroxylated polychlorinated biphenyls by rat liver microsomes. *Environ. Sci. Technol.* **45**, 9590–9596.

Kania-Korwel, I., El-Komy, M. H., Veng-Pedersen, P., and Lehmler, H. J. (2010). Clearance of polychlorinated biphenyl atropisomers is enantioselective in female C57BL/6 mice. *Environ. Sci. Technol.* **44**, 2828–2835.

Kania-Korwel, I., Hornbuckle, K. C., Peck, A., Ludewig, G., Robertson, L. W., Sulkowski, W. W., Espandiari, P., Gairola, C. G., and Lehmler, H. J. (2005). Congener-specific tissue distribution of Aroclor 1254 and a highly chlorinated environmental PCB mixture in rats. *Environ. Sci. Technol.* **39**, 3513–3520.

Kania-Korwel, I., and Lehmler, H. J. (2016a). Chiral polychlorinated biphenyls: Absorption, metabolism and excretion—A review. *Environ. Sci. Pollut. Res. Int.* **23**, 2042–2057.

Kania-Korwel, I., and Lehmler, H. J. (2016b). Toxicokinetics of chiral polychlorinated biphenyls across different species—A review. *Environ. Sci. Pollut. Res. Int.* **23**, 2058–2080.

Kania-Korwel, I., Lukasiewicz, T., Barnhart, C. D., Stamou, M., Chung, H., Kelly, K. M., Bandiera, S., Lein, P. J., and Lehmler, H. J. (2017). Editor's highlight: Congener-specific disposition of chiral polychlorinated biphenyls in lactating mice and their offspring: Implications for PCB developmental neurotoxicity. *Toxicol. Sci.* **158**, 101–115.

Kania-Korwel, I., Shaikh, N. S., Hornbuckle, K. C., Robertson, L. W., and Lehmler, H. J. (2007). Enantioselective disposition of PCB 136 (2,2′,3,3′,6,6′-hexachlorobiphenyl) in C57BL/6 mice after oral and intraperitoneal administration. *Chirality* **19**, 56–66.

Kania-Korwel, I., Zhao, H., Norstrom, K., Li, X., Hornbuckle, K. C., and Lehmler, H. J. (2008). Simultaneous extraction and cleanup of polychlorinated biphenyls and their metabolites from small tissue samples using pressurized liquid extraction. *J. Chromatogr. A* **1214**, 37–46.

Kennedy, M. W., Carpentier, N. K., Dymerski, P. P., and Kaminsky, L. S. (1981). Metabolism of dichlorobiphenyls by hepatic microsomal cytochrome P-450. *Biochem. Pharmacol.* **30**, 577–588.

Kodavanti, P. R., and Curras-Collazo, M. C. (2010). Neuroendocrine actions of organohalogens: Thyroid hormones, arginine vasopressin, and neuroplasticity. *Front. Neuroendocrinol.* **31**, 479–496.

Kodavanti, P. R., Ward, T. R., Derr-Yellin, E. C., McKinney, J. D., and Tilson, H. A. (2003). Increased [^{3}H]phorbol ester binding in rat cerebellar granule cells and inhibition of $^{45}Ca^{2+}$ buffering in rat cerebellum by hydroxylated polychlorinated biphenyls. *Neurotoxicology* **24**, 187–198.

Lee, D. W., Notter, S. A., Thiruchelvam, M., Dever, D. P., Fitzpatrick, R., Kostyniak, P. J., Cory-Slechta, D. A., and Opanashuk, L. A. (2012). Subchronic polychlorinated biphenyl (Aroclor 1254) exposure produces oxidative damage and neuronal death of ventral midbrain dopaminergic systems. *Toxicol. Sci.* **125**, 496–508.

Lehmler, H. J., Harrad, S. J., Huhnerfuss, H., Kania-Korwel, I., Lee, C. M., Lu, Z., and Wong, C. S. (2010). Chiral polychlorinated biphenyl transport, metabolism, and distribution: A review. *Environ. Sci. Technol.* **44**, 2757–2766.

Lehmler, H. J., Robertson, L. W., Garrison, A. W., and Kodavanti, P. R. (2005). Effects of PCB 84 enantiomers on [^{3}H]-phorbol ester binding in rat cerebellar granule cells and $^{45}Ca^{2+}$-uptake in rat cerebellum. *Toxicol. Lett.* **156**, 391–400.

Lesmana, R., Shimokawa, N., Takatsuru, Y., Iwasaki, T., and Koibuchi, N. (2014). Lactational exposure to hydroxylated polychlorinated biphenyl (OH-PCB 106) causes hyperactivity in male rat pups by aberrant increase in dopamine and its receptor. *Environ. Toxicol.* **29**, 876–883.

Lu, Z., Kania-Korwel, I., Lehmler, H.-J., and Wong, C. S. (2013). Stereoselective formation of mono- and di-hydroxylated polychlorinated biphenyls by rat cytochrome P450 2B1. *Environ. Sci. Technol.* **47**, 12184–12192.

Marenich, A. V., Cramer, C. J., and Truhlar, D. G. (2009). Performance of SM6, SM8, and SMD on the SAMPL1 test set for the prediction of small-molecule solvation free energies. *J. Phys. Chem. B* **113**, 4538–4543.

Mariussen, E., and Fonnum, F. (2001). The effect of polychlorinated biphenyls on the high affinity uptake of the neurotransmitters, dopamine, serotonin, glutamate and GABA, into rat brain synaptosomes. *Toxicology* **159**, 11–21.

Mariussen, E., and Fonnum, F. (2006). Neurochemical targets and behavioral effects of organohalogen compounds: An update. *Crit. Rev. Toxicol.* **36**, 253–289.

McGraw, J. E., Sr, and Waller, D. P. (2006). Specific human CYP 450 isoform metabolism of a pentachlorobiphenyl (PCB-IUPAC# 101). *Biochem. Biophys. Res. Commun.* **344**, 129–133.

Milanowski, B., Lulek, J., Lehmler, H. J., and Kania-Korwel, I. (2010). Assessment of the disposition of chiral polychlorinated biphenyls in female mdr 1a/b knockout versus wild-type mice using multivariate analyses. *Environ. Int.* **36**, 884–892.

Nagayoshi, H., Kakimoto, K., Konishi, Y., Kajimura, K., and Nakano, T. (2018). Determination of the human cytochrome P450 monooxygenase catalyzing the enantioselective oxidation of 2,2′,3,5′,6-pentachlorobiphenyl (PCB 95) and 2,2′,3,4,4′,5′,6-heptachlorobiphenyl (PCB 183). *Environ. Sci. Pollut. Res. Int.* **25**, 16420–16426.

Niknam, Y., Feng, W., Cherednichenko, G., Dong, Y., Joshi, S. N., Vyas, S. M., Lehmler, H. J., and Pessah, I. N. (2013). Structure-activity relationship of selected meta- and para-hydroxylated non-dioxin like polychlorinated biphenyls: From single RyR1 channels to muscle dysfunction. *Toxicol. Sci.* **136**, 500–513.

Norstroem, K., and Bergman, A. (2006). Chiral PCB methyl sulfones and their metabolic formation. *Organohalogen Compd.* **68**, 21–24.

Norstrom, K., Eriksson, J., Haglund, J., Silvari, V., and Bergman, A. (2006). Enantioselective formation of methyl sulfone metabolites of 2,2′,3,3′,4,6′-hexachlorobiphenyl in rat. *Environ. Sci. Technol.* **40**, 7649–7655.

Ohta, C., Haraguchi, K., Kato, Y., Endo, T., and Koga, N. (2012). Involvement of rat CYP3A enzymes in the metabolism of 2,2′,3,4′,5′,6-hexachlorobiphenyl (CB149). *Organohalogen Compd.* **74**, 1475–1478.

Pěnčíková, K., Brenerová, P., Svržková, L., Hrubá, E., Pálková, L., Vondráček, J., Lehmler, H.-J., and Machala, M. (2018). Atropisomers of 2,2′,3,3′,6,6′-hexachlorobiphenyl (PCB 136) exhibit stereoselective effects on activation of nuclear receptors in vitro. *Environ. Sci. Pollut. Res. Int.* **25**, 16411–16419.

Pessah, I. N., Cherednichenko, G., and Lein, P. J. (2010). Minding the calcium store: Ryanodine receptor activation as a convergent mechanism of PCB toxicity. *Pharmacol. Ther.* **125**, 260–285.

Peverati, R., and Truhlar, D. G. (2011). Improving the accuracy of hybrid meta-GGA density functionals by range separation. *J. Phys. Chem. Lett.* **2**, 2810–2817.

PharmVar [Pharmacogene Variation Consortium]. 2012. *CYP2A6 allele nomenclature*. Available at: https://www.pharmvar.org/gene/CYP2A6. Accessed July 7, 2019.

PharmVar [Pharmacogene Variation Consortium]. 2013. *CYP2A6 allele nomenclature*. Available at: https://www.pharmvar.org/gene/CYP2A6. Accessed July 7, 2019.

Preston, B. D., Miller, J. A., and Miller, E. C. (1983). Non-arene oxide aromatic ring hydroxylation of 2,2′,5,5′-tetrachlorobiphenyl as the major metabolic pathway catalyzed by phenobarbital-induced rat liver microsomes. *J. Biol. Chem.* **258**, 8304–8311.

Richardson, J. R., and Miller, G. W. (2004). Acute exposure to Aroclor 1016 or 1260 differentially affects dopamine transporter and vesicular monoamine transporter 2 levels. *Toxicol. Lett.* **148**, 29–40.

Schantz, S. L., Moshtaghian, J., and Ness, D. K. (1995). Spatial learning deficits in adult rats exposed to ortho-substituted PCB congeners during gestation and lactation. *Fundam. Appl. Toxicol.* **26**, 117–126.

Schantz, S. L., Seo, B. W., Wong, P. W., and Pessah, I. N. (1997). Long-term effects of developmental exposure to 2,2′,3,5′,6-pentachlorobiphenyl (PCB 95) on locomotor activity, spatial learning and memory and brain ryanodine binding. *Neurotoxicology* **18**, 457–467.

Schecter, A., Colacino, J., Haffner, D., Patel, K., Opel, M., Papke, O., and Birnbaum, L. (2010). Perfluorinated compounds, polychlorinated biphenyls, and organochlorine pesticide contamination in composite food samples from Dallas, Texas, USA. *Environ. Health Perspect.* **118**, 796–802.

Schnellmann, R. G., Putnam, C. W., and Sipes, I. G. (1983). Metabolism of 2,2′,3,3′,6,6′-hexachlorobiphenyl and 2,2′,4,4′,5,5′-hexachlorobiphenyl by human hepatic microsomes. *Biochem. Pharmacol.* **32**, 3233–3239.

Seegal, R. F. (1996). Epidemiological and laboratory evidence of PCB induced neurotoxicity. *Crit. Rev. Toxicol.* **26**, 709–737.

Seegal, R. F., Okoniewski, R. J., Brosch, K. O., and Bemis, J. C. (2002). Polychlorinated biphenyls alter extraneuronal but not tissue dopamine concentrations in adult rat striatum: An in vivo microdialysis study. *Environ. Health Perspect.* **110**, 1113–1117.

Speisky, H., Gomez, M., Burgos-Bravo, F., Lopez-Alarcon, C., Jullian, C., Olea-Azar, C., and Aliaga, M. E. (2009). Generation of superoxide radicals by copper-glutathione complexes: Redox-consequences associated with their interaction with reduced glutathione. *Bioorg. Med. Chem.* **17**, 1803–1810.

Su, G., Liu, X., Gao, Z., Xian, Q., Feng, J., Zhang, X., Giesy, J. P., Wei, S., Liu, H., and Yu, H. (2012). Dietary intake of polybrominated diphenyl ethers (PBDEs) and polychlorinated biphenyls (PCBs) from fish and meat by residents of Nanjing, China. *Environ. Int.* **42**, 138–143.

Thomas, K., Xue, J., Williams, R., Jones, P., and Whitaker, D. 2012. *Polychlorinated Biphenyls (PCBs) in School Buildings: Sources, Environmental Levels, and Exposures*. United States Environmental Protection Agency, Office of Research and Development, National Exposure Research Laboratory.

Uwimana, E., Li, X., and Lehmler, H. J. (2016). 2,2′,3,5′,6-pentachlorobiphenyl (PCB 95) is atropselectively metabolized to

para hydroxylated metabolites by human liver microsomes. *Chem. Res. Toxicol.* **29**, 2108–2110.

Uwimana, E., Li, X., and Lehmler, H. J. (2018). Human liver microsomes atropselectively metabolize 2,2′,3,4′,6-pentachlorobiphenyl (PCB 91) to a 1,2-shift product as the major metabolite. *Environ. Sci. Technol.* **52**, 6000–6008.

Uwimana, E., Maiers, A., Li, X., and Lehmler, H. J. (2017). Microsomal metabolism of prochiral polychlorinated biphenyls results in the enantioselective formation of chiral metabolites. *Environ. Sci. Technol.* **51**, 1820–1829.

Uwimana, E., Ruiz, P., Li, X., and Lehmler, H. J. (2019). Human CYP2A6, CYP2B6 and CYP2E1 atropselectively metabolize polychlorinated biphenyls to hydroxylated metabolites. *Environ. Sci. Technol.* **53**, 2114–2123.

van Meerloo, J., Kaspers, G. J., and Cloos, J. (2011). Cell sensitivity assays: The MTT assay. *Methods Mol. Biol.* **731**, 237–245.

Vetter, W. (2016). Gas chromatographic enantiomer separation of polychlorinated biphenyls (PCBs): Methods, metabolisms, enantiomeric composition in environmental samples and their interpretation. *Isr. J. Chem.* **56**, 940–957.

Voorspoels, S., Covaci, A., and Neels, H. (2008). Dietary PCB intake in Belgium. *Environ. Toxicol. Pharmacol.* **25**, 179–182.

Walker, J. M. (1994). The bicinchoninic acid (BCA) assay for protein quantitation. *Methods Mol. Biol.* **32**, 5–8.

Waller, S. C., He, Y. A., Harlow, G. R., He, Y. Q., Mash, E. A., and Halpert, J. R. (1999). 2,2′,3,3′,6,6′-Hexachlorobiphenyl hydroxylation by active site mutants of cytochrome P450 2B1 and 2B11. *Chem. Res. Toxicol.* **12**, 690–699.

Warner, N. A., Martin, J. W., and Wong, C. S. (2009). Chiral polychlorinated biphenyls are biotransformed enantioselectively by mammalian cytochrome P-450 isozymes to form hydroxylated metabolites. *Environ. Sci. Technol.* **43**, 114–121.

Wayman, G. A., Yang, D., Bose, D. D., Lesiak, A., Ledoux, V., Bruun, D., Pessah, I. N., and Lein, P. J. (2012). PCB-95 promotes dendritic growth via ryanodine receptor-dependent mechanisms. *Environ. Health Perspect.* **120**, 997–1002.

Weigend, F., and Ahlrichs, R. (2005). Balanced basis sets of split valence, triple zeta valence and quadruple zeta valence quality for h to rn: Design and assessment of accuracy. *Phys. Chem. Chem. Phys.* **7**, 3297–3305.

Whitcomb, B. W., Schisterman, E. F., Buck, G. M., Weiner, J. M., Greizerstein, H., and Kostyniak, P. J. (2005). Relative concentrations of organochlorines in adipose tissue and serum among reproductive age women. *Environ. Toxicol. Pharmacol.* **19**, 203–213.

Wong, C. S., Garrison, A. W., Smith, P. D., and Foreman, W. T. (2001). Enantiomeric composition of chiral polychlorinated biphenyl atropisomers in aquatic and riparian biota. *Environ. Sci. Technol.* **35**, 2448–2454.

Wu, X., Duffel, M., and Lehmler, H. J. (2013). Oxidation of polychlorinated biphenyls by liver tissue slices from phenobarbital-pretreated mice is congener-specific and atropselective. *Chem. Res. Toxicol.* **26**, 1642–1651.

Wu, X., Kammerer, A., and Lehmler, H. J. (2014). Microsomal oxidation of 2,2′,3,3′,6,6′-hexachlorobiphenyl (PCB 136) results in species-dependent chiral signatures of the hydroxylated metabolites. *Environ. Sci. Technol.* **48**, 2436–2444.

Wu, X., Kania-Korwel, I., Chen, H., Stamou, M., Dammanahalli, K. J., Duffel, M., Lein, P. J., and Lehmler, H. J. (2013). Metabolism of 2,2′,3,3′,6,6′-hexachlorobiphenyl (PCB 136) atropisomers in tissue slices from phenobarbital or dexamethasone-induced rats is sex-dependent. *Xenobiotica* **43**, 933–947.

Wu, X., and Lehmler, H. J. (2016). Effects of thiol antioxidants on the atropselective oxidation of 2,2′,3,3′,6,6′-hexachlorobiphenyl (PCB 136) by rat liver microsomes. *Environ. Sci. Pollut. Res. Int.* **23**, 2081–2088.

Wu, X., Pramanik, A., Duffel, M. W., Hrycay, E. G., Bandiera, S. M., Lehmler, H. J., and Kania-Korwel, I. (2011). 2,2′,3,3′,6,6′-Hexachlorobiphenyl (PCB 136) is enantioselectively oxidized to hydroxylated metabolites by rat liver microsomes. *Chem. Res. Toxicol.* **24**, 2249–2257.

Yang, D., Kania-Korwel, I., Ghogha, A., Chen, H., Stamou, M., Bose, D. D., Pessah, I. N., Lehmler, H. J., and Lein, P. J. (2014). PCB 136 atropselectively alters morphometric and functional parameters of neuronal connectivity in cultured rat hippocampal neurons via ryanodine receptor-dependent mechanisms. *Toxicol. Sci.* **138**, 379–392.

Zhao, H., Kalivendi, S., Zhang, H., Joseph, J., Nithipatikom, K., Vasquez-Vivar, J., and Kalyanaraman, B. (2003). Superoxide reacts with hydroethidine but forms a fluorescent product that is distinctly different from ethidium: Potential implications in intracellular fluorescence detection of superoxide. *Free Radic. Biol. Med.* **34**, 1359–1368.

Zheng, J., Yu, L.-H., Chen, S.-J., Hu, G.-C., Chen, K.-H., Yan, X., Luo, X.-J., Zhang, S., Yu, Y.-J., Yang, Z.-Y., *et al.* (2016). Polychlorinated biphenyls (PCBs) in human hair and serum from e-waste recycling workers in southern China: Concentrations, chiral signatures, correlations, and source identification. *Environ. Sci. Technol.* **50**, 1579–1586.